Neuroscience Research 105 (2016) 2–18

Contents lists available at ScienceDirect

Neuroscience Research

journal homepage: www.elsevier.com/locate/neures

Characteristics of fast-spiking neurons in the striatum of behaving monkeys

Hiroshi Yamada[a,b,c,d,*], Hitoshi Inokawa[a], Yukiko Hori[a,e], Xiaochuan Pan[f,g], Ryuichi Matsuzaki[h], Kae Nakamura[h,i], Kazuyuki Samejima[f], Munetaka Shidara[c,d], Minoru Kimura[a,f], Masamichi Sakagami[f], Takafumi Minamimoto[a,e,i]

[a] Department of Physiology, Kyoto Prefectural University of Medicine Kawaramachi-Hirokoji, Kamigyo-ku, Kyoto 602-8566, Japan
[b] National Center of Neurology and Psychiatry, 4-1-1 Ogawa-Higashi, Kodaira, Tokyo 187-8502, Japan
[c] Division of Biomedical Science, Faculty of Medicine, University of Tsukuba, Tsukuba, Ibaraki 305-8577, Japan
[d] Graduate School of Comprehensive Human Sciences, University of Tsukuba, Tsukuba, Ibaraki 305-8577, Japan
[e] Department of Molecular Neuroimaging, Molecular Imaging Center, National Institute of Radiological Sciences, Chiba 263-8555, Japan
[f] Brain Science Institute, Tamagawa University, 6-1-1, Tamagawa-Gakuen, Machida, Tokyo 194-8610, Japan
[g] Institute for Cognitive Neurodynamics, East China University of Science and Technology, Shanghai 200237, China
[h] Department of Physiology, Kansai Medical University, Shin-machi, Hirakata city, Osaka 570-1010, Japan
[i] Precursory Research for Embryonic Science and Technology, Japan Science and Technology Agency, 4-1-8 Honcho Kawaguchi, Saitama 332-0012, Japan

ARTICLE INFO

Article history:
Received 25 December 2014
Received in revised form 6 October 2015
Accepted 7 October 2015
Available online 23 October 2015

Keywords:
Basal ganglia
Inhibitory interneuron
Monkey
Reward

ABSTRACT

Inhibitory interneurons are the fundamental constituents of neural circuits that organize network outputs. The striatum as part of the basal ganglia is involved in reward-directed behaviors. However, the role of the inhibitory interneurons in this process remains unclear, especially in behaving monkeys. We recorded the striatal single neuron activity while monkeys performed reward-directed hand or eye movements. Presumed parvalbumin-containing GABAergic interneurons (fast-spiking neurons, FSNs) were identified based on narrow spike shapes in three independent experiments, though they were a small population (4.2%, 42/997). We found that FSNs are characterized by high-frequency and less-bursty discharges, which are distinct from the basic firing properties of the presumed projection neurons (phasically active neurons, PANs). Besides, the encoded information regarding actions and outcomes was similar between FSNs and PANs in terms of proportion of neurons, but the discharge selectivity was higher in PANs than that of FSNs. The coding of actions and outcomes in FSNs and PANs was consistently observed under various behavioral contexts in distinct parts of the striatum (caudate nucleus, putamen, and anterior striatum). Our results suggest that FSNs may enhance the discharge selectivity of postsynaptic output neurons (PANs) in encoding crucial variables for a reward-directed behavior.

1. Introduction

The activity of various classes of interneurons regulates the information flow in the brain subserving cognition and volition. Striatum, an input stage of the basal ganglia, is involved in a wide range of reward-directed behaviors, and its output has been suggested to be under the control of various classes of interneurons (Kawaguchi et al., 1995). Cholinergic signal mediated by cholinergic interneurons has been shown to modulate the activity of the striatal output neurons (Goldberg et al., 2012; Schulz and Reynolds, 2013). Activity of the output neurons and cholinergic interneurons in behaving animals has been well examined in relation to learning and performance in reward-directed behaviors (Aosaki et al., 1994a; Balleine et al., 2007; Cai et al., 2011; Garenne et al., 2011; Jog et al., 1999; Kawagoe et al., 1998; Lau and Glimcher, 2008; Morris et al., 2004; Samejima et al., 2005; Schultz et al., 2003; Yamada et al., 2004, 2007), while the medium spiny projection neurons (output neurons) and the cholinergic interneurons have been electrophysiologically characterized as PANs and TANs (tonically active neurons), respectively (Apicella et al., 1991; Inokawa et al., 2010; Kimura, 1990). Little is known, however, about how the striatal inhibitory interneurons organize the striatal outputs in behaving animals, especially in close primate relatives to human, macaque monkeys.

* Corresponding author at: Division of Biomedical Science, Faculty of Medicine, University of Tsukuba, 1-1-1 Tennodai, Tsukuba, Ibaraki 305-8577, Japan.
Tel.: +81 29 853 6013; fax: +81 29 853 6013.
E-mail address: h-yamada@md.tsukuba.ac.jp (H. Yamada).

http://dx.doi.org/10.1016/j.neures.2015.10.003

Beyond these two classes of striatal neurons, parvalbumin-containing GABAergic interneurons have been identified in vitro based on their histochemical properties and morphologies (Kawaguchi et al., 1995). This class of interneurons has been electrophysiologically characterized as FSNs in rodent slice preparation (Tepper et al., 2004; Wilson, 2007). FSNs possess perisomatic synapses with a powerful inhibitory influence on medium spiny projection neurons (Koos and Tepper, 1999). Neuronal activity of FSNs in reward-directed behaviors has been examined in small number of rodent studies, suggesting that they represent information for actions and outcomes (Gage et al., 2010; Lansink et al., 2010; Schmitzer-Torbert and Redish, 2008). However, to the best of our knowledge, no study has examined the role of FSNs in organizing striatal outputs during reward-directed behaviors in monkeys. It is largely because FSN constitutes a minority of cell classes in the striatum (Kawaguchi et al., 1995), and thus, only tiny amount of sample data could be obtained in a single study. Given this limitation, it is challenging to elucidate the inhibitory mechanism of FSNs on the regulation of striatal outputs, which are presumably embedded across distinct functional territories of the striatum.

In the present study, we aimed to understand how FSNs organize striatal outputs during reward-directed behaviors in monkeys. To overcome the above-mentioned difficulty, we accumulated and analyzed single neuron activity in four independent experiments, in which activity of PANs has already been reported under various behavioral contexts. We differentiated FSNs from other neurons based on the spike shapes recorded extracellularly in the striatum of behaving monkeys. We addressed the two critical issues to examine the role of FSNs in organizing striatal outputs: (i) How are FSNs in the striatum of behaving monkeys involved in guiding their actions toward reward outcomes? And (ii) How is the activity of FSNs distinct from that of PANs, while the striatal output would be shaped by inhibition of FSNs? We asked these questions in distinct parts of the striatum in view of cortico-basal ganglia functional loops (e.g., the motor loop, associative loop, and limbic loop). Our results suggest that FSNs may enhance the discharge selectivity of postsynaptic output neurons (PANs) during reward-directed behaviors.

2. Materials and methods

The data obtained from the four independent experiments were used in the present study. Table 1 is the summary of the experiments including their reference numbers (#1 to #4), behavioral task used, the number of monkeys, recording sites, and paper in which the results of PANs have been reported. In this study, we briefly describe each experiment in terms of behavioral task, recording methods, and the specific data analysis used. Other details have been described previously (see references in Table 1). All experimental procedures were carried out in accordance with the Guide for the Care and Use of Laboratory Animals (National Research Council of the National Academies in the USA) and were approved by the Animal Care and Use Committee of the Kyoto Prefectural University of Medicine (Exps. 1 and 2), Tamagawa University (Exp. 3), and Kansai Medical University (Exp. 4).

2.1. Subjects and behavioral tasks

2.1.1. Experiment 1

Single neuron activity was recorded from the caudate nucleus and putamen of two monkeys (monkeys RO and TN), while they performed a task using the arm contralateral to the recording hemisphere to obtain multiple rewards through a series of choices. All details regarding analyses of the monkeys' behavior and activity of the PANs ($N = 292$) have been reported previously (Yamada et al., 2011). Here we analyzed the activity of 280 PANs for which spike shape data were available. The activities of FSNs and TANs in this experiment have not been reported elsewhere.

Multistep choice task. The monkeys performed multistep choice tasks using a trial-and-error approach. After illumination of the start light-emitting diode (LED), the monkeys depressed the illuminated start button. Then, three target LEDs were turned on; the monkeys were required to keep the start button depressed for another moment until the small, red Go LED was turned off (GO), release the start button, and depress one of the three illuminated target buttons within 3 s. If a reward target button was depressed, a high-tone beep (1 kHz) sounded with a delay of 0.9–1.0 s as positive feedback, and reward water was then delivered. If a no-reward target button was depressed, a low-tone beep (0.3 kHz) sounded as negative feedback and no reward was given.

If the monkeys chose the no-reward target in the first step, the second step of the search trial began with the illumination of the start LED 5 s (inter-trial interval; ITI) after the end of the first step. The three targets were illuminated again and the monkeys chose the target. The monkeys remembered the no-reward target chosen during the first step and made another choice between the two remaining target buttons in the second step. If they depressed another no-reward target button, the negative feedback beep sounded and the third step started. They then had to remember the previous two no-reward targets and depress the remaining single target button. Once the monkeys depressed the reward target button in any step of the search trial, the same button was used again as the reward target button in the next repeat trial. The monkeys received a water reward once during the search trials, and once (monkey RO) or twice (monkey TN) during the repeat trials. To instruct the monkeys of the termination of a single series of choices, all four green LEDs were simultaneously flashed for 1 s at 2 s after the end of the final repeat trial.

2.1.2. Experiment 2

Single neuron activity was recorded from the putamen while one monkey was engaged in a task using its arm to obtain rewards. All details regarding analyses of the monkeys' behavior and activity of the PANs have been previously reported (Hori et al., 2009). The activities of FSNs and TANs during this task have not been reported elsewhere.

GO–NOGO button-press task with asymmetric rewards. The monkeys faced a panel in which a rectangular hold button and two instruction buttons were embedded. When the monkey depressed the hold button for 0.2–0.6 s, one of the two instruction buttons was illuminated yellow as a cue stimulus. After some delay, its color turned to either green or red, instructing GO or NOGO action, respectively. After the GO instruction, the monkey released the hold button and depressed the illuminated target button within 3 s. After the NOGO instruction, the monkey kept depressing the hold button for another moment. Combinations of either a large water reward (0.3 ml, +R) after the successful GO trials and a small water reward (0.1 ml, −R) after the successful NOGO trials or vice versa were run in single block of 60–120 correct trials. The occurrence of large- and small-reward trials was not predictable (the average probability was 0.5). A high (1 kHz) or a low (0.3 kHz) tone was sounded after a correct behavioral reaction, which was followed by a large reward (LR) or a small reward (SR), respectively.

2.1.3. Experiment 3

Single neuron activity was recorded from the anterior part of the striatum while one monkey was engaged in an eye movement task to obtain rewards. All details regarding analyses of the monkey's behavior and the activity of PANs have been reported previously (Pan et al., 2014). TANs were classified online but were

Table 1
List of all experiments and articles in which activity of PANs has been reported by behavioral task.

Experiment #	Behavioral task	Number of monkeys	Number of neurons classified (% total)				Number of neurons unclassified	Recording site	Paper reported
			FSN	PAN	TAN	Total			
1	Multi-step choice	2	31 (5)	280* (45)	318 (50)	629	–	Cd.N/PUT	(Yamada et al., 2013a, 2011)
2	*GO-NOGO button-press with asymmetric rewards*	1	8 (4)	137* (64)	68 (32)	213	–	PUT	(Hori et al., 2009)
3	Sequential paired-association	1	3 (2)	152* (98)	–	155	–	Cd.N/PUT	(Pan et al., 2014)
4	*Visually guided saccade with asymmetric rewards*	2	–	–	–	–	275*	Cd.N/vSTR	(Nakamura et al., 2012)
Total		6	42 (4.2)	569 (57.1)	386 (38.7)	997 (100)	275		

Asterisks indicate neuron types on which the result has been reported previously. Cd. N, caudate nucleus; PUT, putamen, vSTR, ventral striatum.

not recorded. The activity of FSNs during this task has not been reported elsewhere.

Sequential paired-association task. A monkey learned two visual stimulus–stimulus associative sequences (A1 –> B1 –> C1 and A2 –> B2 –> C2, where A1, B1, C1, A2, B2, and C2 are six different visual stimuli). Then, the monkey learned an asymmetric reward schedule in reward instruction trials, in which one stimulus (C1 or C2) was paired with a large reward (LR, 0.4 ml water) and another stimulus (C2 or C1) with a small reward (SR, 0.1 ml water). Reward instruction trials and sequential paired-association trials (SPATs) were arranged in a block; the reward instruction trials were presented first, followed by the SPATs. The asymmetric reward schedules for reward instruction trials and SPATs were the same in each block: if C1 had been paired with the LR and C2 with the SR in the reward instruction trials, the sequence A1 –> B1 –> C1 would lead to the LR, while the sequence A2 –> B2 –> C2 would lead to the SR, and vice versa.

2.1.4. Experiment 4

Single neuron activity was recorded from caudate nucleus while two monkeys were engaged in an eye movement task to obtain rewards. All details regarding analyses of monkey's behavior and activity of the striatal neurons have been reported previously (Nakamura et al., 2012). TANs were classified online but were not included in the analyses.

Visually guided saccade task with asymmetric rewards. Monkeys performed a visually guided saccade, from the central fixation point to the target presented to either left or right. The sequence for the target position was pseudorandom, while the reward size was associated with the target position.

2.2. Data recordings

Conventional electrophysiological techniques were used to record the single neuron activity. Band pass filters (Exp. 1: 50 Hz to 3 kHz, Nihonkoden AB-611J; Exp. 2: band pass, 50 Hz to 3 kHz, Nihonkoden AB-611J; Exp. 3: band pass, 100 Hz to 8 kHz, Plexon MAP; Exp. 4: band pass, 150 Hz to 3 kHz, Nihonkoden MEG-5100) were kept constant throughout the experiment because spike shapes depend on the setting of the band-pass filters (Mizuhiki et al., 2012). In Exps. 1 and 2, the action potentials of single neurons were isolated and sampled at 25 or 50 kHz using a spike sorter with a template-matching algorithm (MSD, Alpha Omega). In Exp. 3, the Plexon system was used to discriminate individual spike waveforms online. The onset times of the action potentials were recorded on a laboratory computer together with the task events.

2.3. Classification of neuron type

In each experiment FSNs (presumed parvalbumin-containing GABAergic interneurons) were differentiated from PANs (presumed projection neurons) and TANs (presumed cholinergic interneurons) by their spike width (i.e., the width at the half max of the negative peak amplitude and the width of spike from peak to valley). We classified FSNs as the neurons in one cluster exhibiting narrow spike waveforms (Gage et al., 2010). Thereafter, PANs and TANs were classified by their background discharge rates and firing patterns in addition to the spike width. PANs usually showed low spontaneous firing rates (<2 spikes/s) and phasic discharges in relation to one or more task events (Kimura et al., 1990), while TANs showed irregular tonic firing at around 3.0–8.0 Hz (Inokawa et al., 2010; Kimura et al., 1990).

2.4. Data analysis

Inter-spike interval (ISI) distribution was obtained from the data in each neuron through all recording periods. A peak in the ISI distribution was detected in each neuron using a 10 ms bin. The average firing rates were estimated during the ITI. ITIs were defined as a 4 s window before the start LED onset (Exp. 1), a 3 s window 500 ms before the start LED onset (Exp. 2) and a 1 s window before the onset of the fixation point (Exp. 3), respectively. During the task trials, the average firing rates were estimated for a window from the onset of the start LED to 2 s after the feedback beeps (Exps. 1 and 2) and a window from the onset of the fixation point to the reward onset (Exp. 3), respectively. A width of half-peak activation in the peristimulus histogram (PSTH) was estimated as follows: Histograms were smoothed with a Gaussian kernel. We detected the maximum activation in each neuron by constricting the PSTH at each behavioral event. Then, the duration of activity above the half-peak activation was estimated as the width of half-peak activation.

A significant change in the discharge rate of FSNs and PANs was determined by Wilcoxon two-sample test by comparing the discharge rate during each task period with the background rate during the ITI period, using Bonferroni correction for an adjustment made to P values at $P < 0.05$. For example, comparisons in experiment 1 were made during each of the five task periods: *start period* (for 1000 ms preceding and 300 ms following the depression of the start button), *pre-GO period* (for 600 ms preceding the GO signal), *target choice period* (for 300 ms preceding and following the depression of the target button), *pre-feedback period* (for 600 ms preceding the feedback beeps), and *post-feedback period* (for 2000 ms following the feedback beeps).

In experiment 1, the following analyses were conducted as described in Yamada et al. (2011). The influence of reward probability, search or repeat trial, positive and negative outcome feedback,

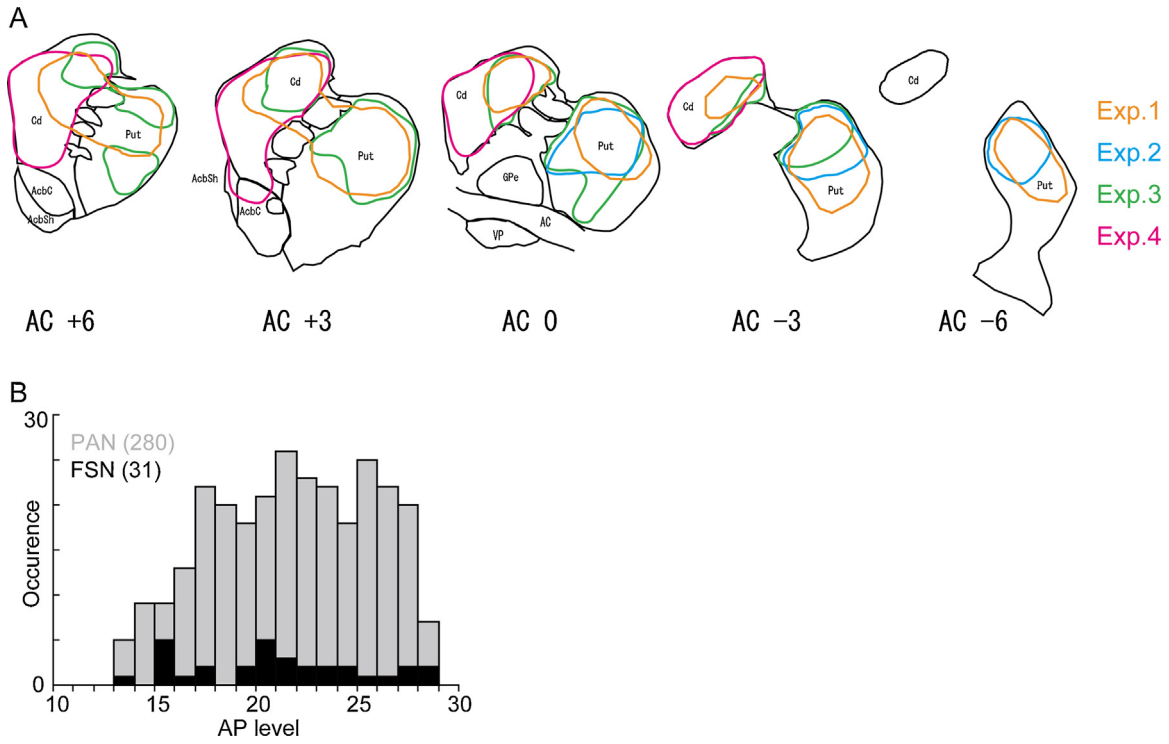

Fig. 1. Summary of the recording sites in the striatum. (A) Approximate area of the striatal neurons recorded in each experiment according to the anterior commissure (AC) level; Exp. 1, yellow; Exp. 2, blue; Exp. 3, green; Exp. 4, magenta. The recorded area was adjusted to the atlas in Paxinos Rhesus Monkey (http://scalablebrainatlas.incf.org/main/index.php). (B) Occurrence of FSNs and PANs according to the anterior–posterior level of the striatum in experiment 1.

and target choice on neuronal discharge rate was examined using multiple regression analysis. In short, neuronal discharge rates (F) were fitted using the following model:

$$F = b_0 + b_p\,\text{Probability} + b_s\,\text{Search-Repeat} + b_t\,\text{Target} + \text{error},$$

where b_0 and error are the intercept and residual, respectively; "Probability" is the average reward rate in each step of search and repeat trials, for monkey RO (search: 0.33, 0.50, and 0.89 and repeat: 0.96), and for monkey TN (search: 0.32, 0.49, and 0.82 and repeat: 0.93 and 0.96); "Search-Repeat" took scalar values (1, 0) in search and repeat trials, respectively; "Target" took scalar values (1, 0, −1) for the three target options, and these values were assigned depending on the average discharge rates for each target. For neuronal discharge rate during the post-feedback period, we used the following model:

$$F = b_0 + b_p\,\text{Probability} + b_s\,\text{Search-Repeat} + b_t\,\text{Target} + b_f\,\text{Feedback} + \text{error},$$

where "Feedback" took scalar values (1, 0) in reward and no-reward trials. If the regression coefficients were not zero at $P < 0.05$, the discharge rates were regarded as being significantly modulated by that variable. Neurons were categorized as "Probability" type with significant b_p; "Search-Repeat" type with significant b_s and insignificant b_p; "Feedback" type with significant b_f and insignificant b_p and b_s; and "Target" type with significant b_t and insignificant b_p, b_s, and b_f. Neurons with significant b_p and b_s were categorized as "Combo" type (significant b_p and b_s, with the same signs).

2.5. Histology

At the end of the recording in Exps. 1 and 2, small electrolytic lesions were made in the caudate nucleus and/or putamen. Electrode tracks through the striatum were reconstructed on the histological sections using the electrolytic lesion marks as reference points, and the recording sites of striatal neurons were identified.

3. Results

3.1. Classification of FSNs and other neurons based on spike width

We studied total 1272 neurons recorded extracellularly from the striatum of behaving monkeys in four independent experiments. Neurons were recorded from a large part of the striatum (caudate nucleus, putamen, or anterior striatum, Fig. 1A), while monkeys performed arm or saccadic movement to obtain rewards.

We classified the neurons into FSNs, PANs, and TANs based on the spike shapes. For classification of striatal neurons, we applied the procedures previously used in rat studies (Bartho et al., 2004; Gage et al., 2010). A scatter plot of peak width (i.e., width at the half max of the negative peak amplitude) against peak-to-valley width (i.e., time from negative peak to valley) for all neurons formed two clusters in experiments 1–3 (Fig. 2A–C). We classified FSNs as the neurons in one cluster exhibiting narrow spike waveforms (Fig. 2A, inset), which resembled those observed in striatal FSNs in behaving rats (Gage et al., 2010). FSNs amounted to approximately 4% (42/997) of all neurons in experiments 1–3 (Table 1). Another cluster of neurons with wider spike waveforms was further categorized into either TANs or PANs according to the conventional criterion of whether they showed the irregular tonic firing or not (Kimura et al., 1990). In contrast, the scatter plot for the data in experiment 4 formed two clusters that were not clearly separated from each other (Fig. 2D). Since FSNs were not identified in experiment 4, the data were excluded from further analyses. Note that the spike width values largely varied across experiments (e.g., half-max width in ms; 0.2–0.8, 0.1–0.6, 0.1–0.3, and 0.1–0.5, in Exps. 1–4, respectively). The divergence of the spike width was probably due to the different amplifier filter settings used (see Section 4).

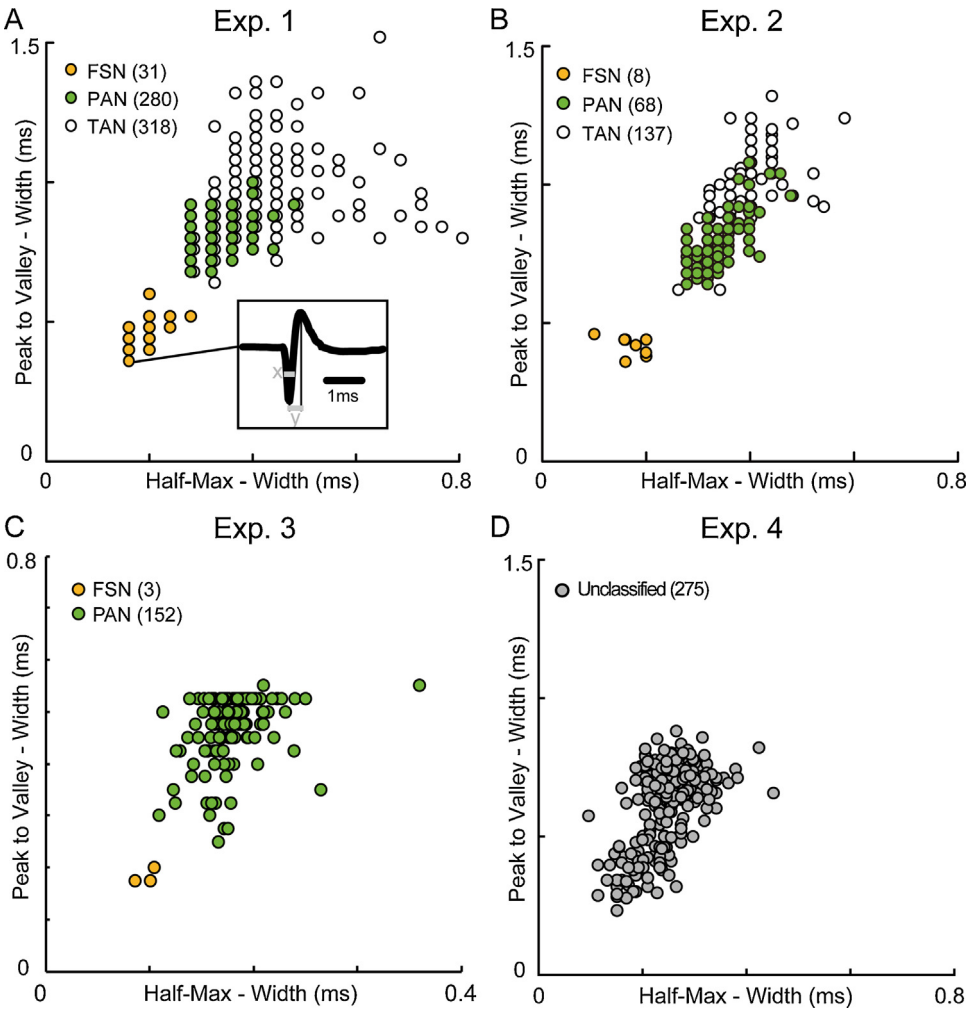

Fig. 2. Classification of FSNs based on spike waveform. (A–D) Scatter plots of mean spike waveform durations (x, the width at the half max of the negative peak amplitude; y, the width from peak to valley, see inset in A) for each neuron in experiments 1–4, respectively. FSNs were defined as the neurons in one cluster exhibiting narrow spike waveforms (orange). Neurons in the other cluster with wider spike waveforms were further classified into TANs (white) and PANs (green) based on the conventional definition (i.e., whether irregular tonic firing occurred or not). Gray means unclassified neurons. The number of neurons classified is shown in parenthesis. The activity of TANs was not recorded in Exps. 3 and 4. Our classification method cannot be applied to the data in Exp. 4 (D).

We did not find any localization bias of FSNs and PANs in the striatum. For example, there was no predominant bias of the recorded location on the anterior–posterior level in experiment 1 (Fig. 1B, two sample t-test, $P = 0.36$). There was no predominant bias among caudate nucleus and putamen (seven FSNs and 113 PANs vs. 24 FSNs and 167 PANs, Fisher's exact probability test, $P = 0.08$).

3.2. Comparison of basic firing properties between FSNs and PANs

We analyzed the activity of FSNs and PANs in three independent behavioral tasks: multistep choice task (Exp. 1, Fig. 3A and B), GO–NOGO button-press task with asymmetric rewards (Exp. 2, Fig. 3C and D), and sequential paired-association task (Exp. 3, Fig. 3E–G). An example of FSN activity in experiment 1 (Fig. 4A) showed tonic firing at around 30 Hz in most task periods, with a phasic increase and decrease of discharges for some task events (at hold button press and at hold button release followed by target button press; see Fig. 3A for the sequence of task events). A second example of FSN activity showed a phasic increase in discharges during hold depression and increased activity toward hold release followed by decreased firing during monkeys' arm movement to choose the target button (Fig. 4B). In contrast, PANs typically show a phasic increase in discharges at some task events without tonic baseline firings as exemplified in Fig. 4C. Similarly, some FSNs showed phasic discharges during arm movements (hold press and release, Fig. 4D) unaccompanied by tonic discharges. To visualize these discharge changes during the task, normalized firing rates for each neuron in FSNs and PANs in Exp. 1 were displayed in color-coded histograms and aligned by the hold press and the target press (Fig. 4E). A considerable proportion of FSNs showed tonic firing at a rate more than half maximum (i.e., pink) in most of the task periods (Fig. 4E, top) and sometimes showed phasic increase or decrease of their discharges related to task events. On the contrary, PANs did not show tonic firings but increased their discharge phasically in a narrow time window (Fig. 4E, bottom).

We examined the average firing rates of FSNs and PANs during ITI and task trial (Fig. 5). Regarding the small sample size of individual FSNs, we examined the data in each independent experiment as well as the combined data. Firing rate of FSNs did not differ between ITI and task trial in two of three experiments (Fig. 5A and C, paired t-test, $P > 0.05$) and in the combined data (Fig. 5D, two-way ANOVA, period × experiment; period, $P = 0.22$, interaction, $P = 0.56$). In contrast, PANs showed higher firing rates during task trial as compared to ITI in all three experiments (paired t-test, $P < 0.001$) as well as in the combined data (Fig. 5D, period, $P < 0.001$), reflecting almost no firing during ITI, but phasic activation related to the

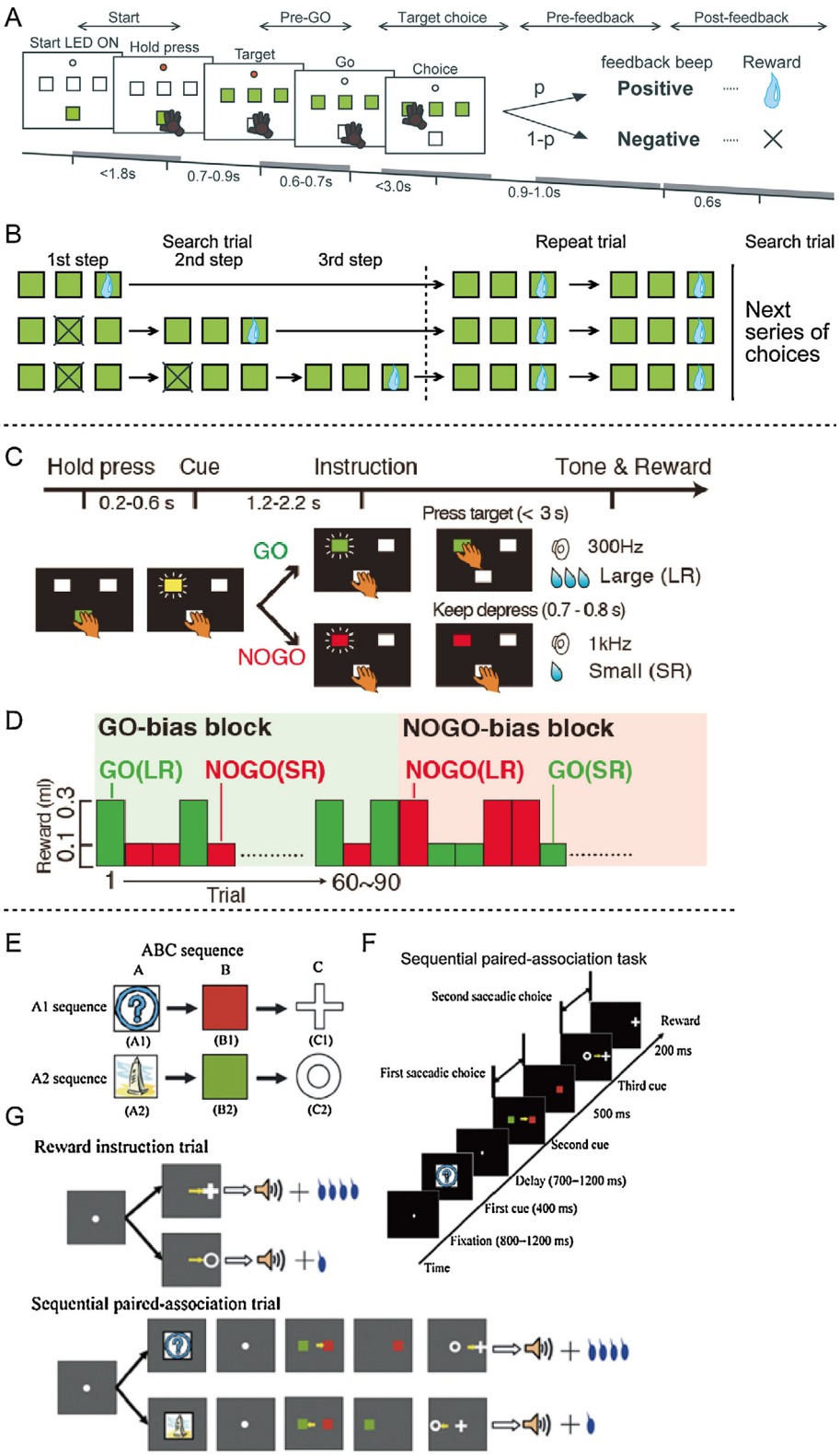

Fig. 3. Behavioral tasks. (A) and (B) Multistep choice task used in Exp. 1. (A) Sequence of events in a single trial. Gray bars on the time line indicate the task periods used to analyze neuronal activity: start, pre-Go, target choice, pre-feedback, and post-feedback. (B) Three examples of decisions made by monkey TN to find a reward target throughout a series of choices. In these examples, the right target was rewarded for the first, second, and third steps of search trials. Once the monkey depressed a reward target button, the same button was used again as the reward target button in the following repeat trials. Reward and no-reward outcomes are illustrated as in A. (C) and (D) GO–NOGO button-press task with asymmetric rewards used in Exp. 2. (C) Sequence of events occurring during a GO-bias block in which GO trials were followed by a large reward (LR), while NOGO trials were followed by a small reward (SR). (D) GO-biased and NOGO-biased blocks consisted of 60–90 successful trials. Colored bars indicate the trial type sequence (green, GO; red, NOGO) and reward size (tall, LR; short, SR) in each block. (E)–(G) Sequential paired-association task used in Exp. 3. (E) An example of two associative sequences (ABC sequences) learned by monkeys. (F) Schematic illustration of a sequential paired-association trial (SPAT). The monkey made a choice by a saccadic eye movement, as indicated by small yellow arrows. There were two choices in the trial; the first choice was from stimulus A to B, and the second choice was from B to C. (G) An asymmetric stimulus–reward contingency was introduced in reward instruction trials and used in the subsequent SPATs in one block.

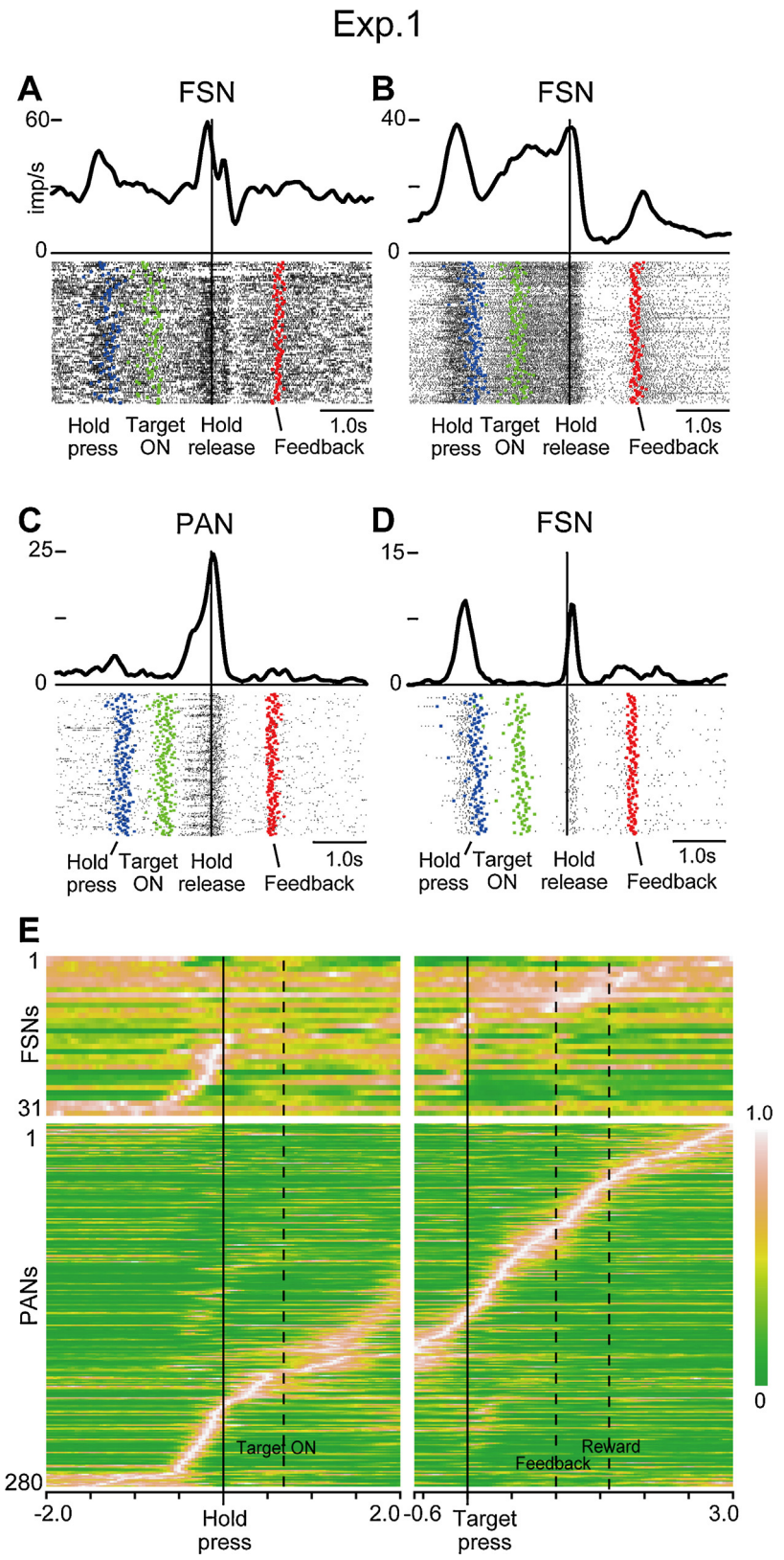

Fig. 4. Task-related activity changes in FSNs and PANs. (A) and (B) Two examples of FSN activity during multistep choice task in experiment 1. Rasters and histograms are aligned at the time of hold button release (hold release) when followed by target button choice. Blue, green, and red marks in the raster indicate the time of hold press, onset of target, and feedback beep, respectively. (C) Same as A, but for an example of PAN activity. (D) Same as A, but for another example of FSN activity. (E) Event-related activity of FSNs ($N = 31$) and PANs ($N = 280$) in experiment 1. Firing rates are normalized (max = 1) and aligned at the time the monkey depressed the hold button (left) and the target button (right), respectively. All histograms (40-ms bins) are smoothed with a Gaussian kernel (40 ms).

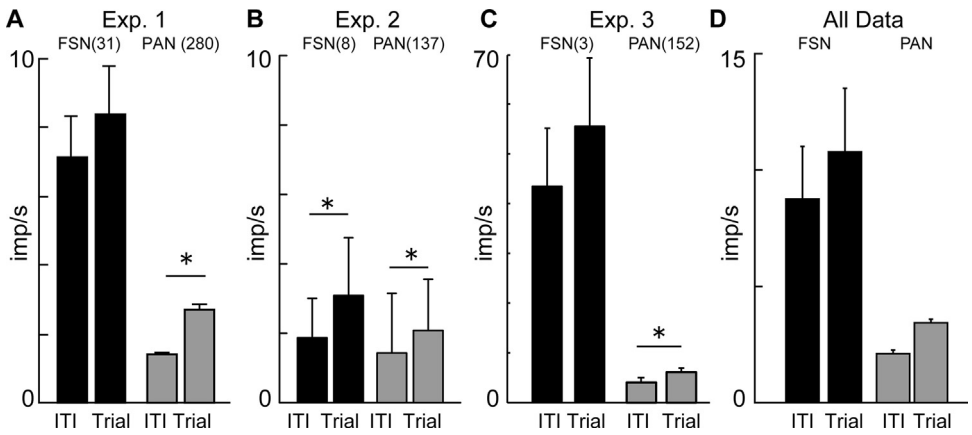

Fig. 5. Average discharge rates of FSNs and PANs. (A)–(D) Average firing rate of FSNs and PANs during inter-trial interval (ITI) and task trial (Trial) in Exp. 1–3 and combined data, respectively. Asterisk in A–C indicates statistical significance at $P < 0.01$ using paired *t*-test.

performance of one or more task events. The overall firing rate during recording periods was significantly higher in FSNs than in PANs (three-way ANOVA, period × experiment × neuron type; neuron type, $P < 0.001$). Thus, FSNs and PANs in the striatum of behaving monkeys possess distinct properties with regard to the average firing rates.

Next, we examined temporal profiles of the task-related activity changes in two neuron subtypes. To assess the duration of activity change, we measured width of half-peak activation in each neuron in experiment 1. An example of FSN activity showed its discharge peak after the target button depression, for duration of 3.6 s (Fig. 6A). The half-peak duration of FSNs was widely distributed, ranging from 0 to 5 s, with the mean 2.74 ± 0.41 s (mean ± S.E.), and was significantly longer than that of the PANs (1.23 ± 0.66, Wilcoxon two-sample test, $P < 0.001$; Fig. 6B). Thus, FSNs showed a longer duration of increased firing rates as compared to PANs whose phasic firing occurred in a narrow time window.

The longer duration of activity change in FSNs often covered several task events. Among the five task periods in experiment 1 (start, pre-GO, choice, pre-feedback and post-feedback), FSNs showed significantly different activity compared to ITI in more periods (on average, 3.8 task periods) than PANs (average, 2.4 task periods; two-sample *t*-test, $p < 0.001$). Both increase and decrease in FSN activity were observed. For each of the five task periods, about a half of FSNs showed significantly higher discharge rates (facilitation), whereas about a quarter of the neurons exhibited lower discharge rates (suppression, Fig. 6C). Proportions of the facilitation and suppression were similar across task periods (chi-squared test, $p = 0.67$). Thus, facilitation, not suppression, primarily occurred across many task periods in FSNs.

We further examined the characteristics of temporal firing properties in FSNs and PANs. We detected the peak of the ISI histogram in each neuron (e.g., Fig. 7A inset, 45 ms) and constructed distribution of ISI peaks for FSNs and PANs (Fig. 7). The ISI peak distribution of FSNs was characterized by a relative scarcity of the short ISI peaks as compared to the shorter ones of the PANs. ISI peaks of FSNs were larger than that of PANs in each experiment (e.g., Fig. 7A; Wilcoxon two-sample test, $P < 0.001$) as well as in the combined data (two-way ANOVA, cell type × experiment; cell type $P < 0.001$). Indeed, 90% of the ISI peaks in FSNs occurred for more than 20 ms, while 75% of those in PANs occurred within 20 ms in experiment 1. Thus, the FSN firing was more regular and less bursty as compared to that of the PANs.

3.3. Encoding actions and outcomes under various behavioral contexts

Despite the dissimilar basic firing profiles, we found similarity in activity modulation between FSNs and PANs recorded in large parts of the striatum during various kinds of reward-directed behavior. In this section, we describe how FSNs change their activity depending on actions and outcomes, the two critical components for reward-directed behavior, and compare with the activity of PANs. Characteristics of activity modulation in PANs in each experiment have been reported previously (Table 1).

During value-based decision-making, neuronal activity was recorded from caudate nucleus and putamen in experiment 1 (Fig. 1, yellow). Monkeys performed the multistep choice task in which average probability of choosing a rewarding target increased through the trial-and-error search (Fig. 3B, search trials), and then remained high when repetition of the same choice (repeat trials) was required. We found that FSNs showed modulation of discharge rates by actions (i.e., target choice) and/or outcome feedback. An example activity of FSNs shown in Fig. 8A exhibited the sustained discharges just before hold button release and responded to the target choice (hold release to target press) by facilitation followed by suppression. This phasic activity depended on the chosen targets, higher for the middle target choice and lower for the right target choices. Activity of FSNs was also modulated by the outcome feedback. An example FSN had discharged after positive feedback (i.e., reward, Fig. 8B), and another showed increased activity after negative feedback (i.e., no reward, Fig. 8C). The multiple regression analysis revealed that the activities of these example FSNs were modulated by the chosen target (Fig. 8A, $P = 0.002$) and outcome feedback (Fig. 8B, $P = 0.001$; Fig. 8C, $P < 0.001$). Since these activities were not modulated by either reward probability or search–repeat trials ($P > 0.05$ in all examples), these FSNs exclusively encoded the chosen targets and outcome feedback, respectively.

The selective coding of the chosen targets (target type) was the most prominent feature of FSNs and frequently observed during preparation (pre-GO period) and execution (target choice period) of target choices (Fig. 8D, gray bars). The proportion of the target type observed through task periods was not different between FSNs and PANs (Chi-squared test, $P = 0.80$). Thus, the predominant coding of the target choice by FSNs was similar to that by PANs in the striatum. In both FSNs and PANs, the selective coding of outcome feedback (feedback type) was also predominantly observed (Fig. 8A, yellow bars), and there was no significant difference in the proportion of the feedback type (Fisher's exact probability test,

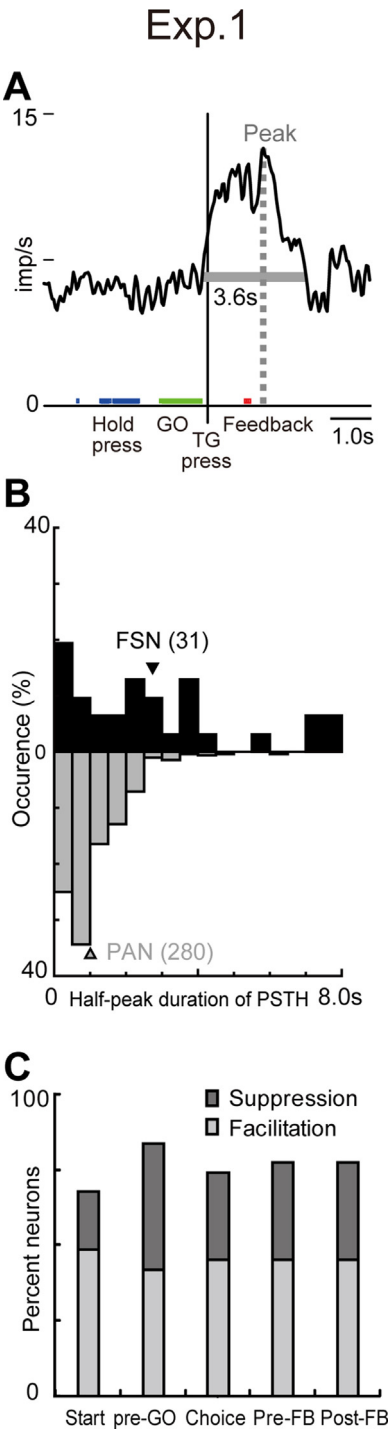

Fig. 6. Temporal profiles of task-related activity changes in FSNs and PANs. (A) Estimation of the half-peak activity duration for an example FSN. (B) Histograms showing duration of half-peak activation for individual neurons in FSNs (black, upper) and PANs (gray, lower). Triangles indicate means. (C) Percentage of FSNs showing increased (facilitation, light gray) and decreased (suppression, dark gray) discharge in each task period compared to discharges in the ITI period. Pre-FB and post-FB indicate pre-feedback and post-feedback periods, respectively.

$P = 0.07$). In addition, there was no significant difference in the proportion of neurons encoding positive and negative outcome feedback between FSNs and PANs (FSNs, four positive vs. 13 negative feedback types; PANs, 20 positive vs. 27 negative feedback types; Fisher's exact probability test, $P = 0.24$). Thus, predominant coding of actions and outcomes was similarly observed between FSNs and PANs in the striatum.

In addition to the target choice and feedback coding, selective coding of other variables related to decision-making, such as reward probability or task-specific strategy as in search–repeat trials, was also observed in FSNs, in similar proportion to PANs (Fig. 8D, chi-squared test; probability type (blue), $P = 0.17$; search–repeat type (pink), $P = 0.99$). Combo type (green), which is the combination of the reward probability and search–repeat strategy, was also observed in a small proportion of FSNs similar to that of PANs. Thus, both FSNs and PANs in the caudate nucleus and putamen encoded actions and outcomes similarly in terms of proportion of neurons.

We also observed the similarity between FSNs and PANs in the putamen in encoding actions and outcomes during reward-directed arm movement, while the putamen is suggested to be involved in acquiring action–reward associations and guidance of actions toward rewards. In experiment 2, neuronal activity was recorded from the posterior part of the putamen (i.e., motor striatum, Fig. 1, blue), while a monkey performed a GO–NOGO button-press task (Fig. 3C and D), during which, action type, a button press (GO) or withholding of the action (NOGO), was associated with reward size (LR or SR). One example activity of FSN showed gradual increase in discharges toward the action–reward instruction and then stopped firings (Fig. 9A). The activity was significantly stronger in the GO(LR)–NOGO(SR) blocks (Wilcoxon two-sample test, $P < 0.001$). In eight FSNs, five showed the pre-instruction activity. Likewise, about 15% of PANs showed the pre-instruction activity, most of which differentiated blocks (Hori et al., 2009). Another example showed post-instruction activity depending on the combination of action and reward size; the phasic discharge after GO instruction was higher in LR than in SR trials, whereas a relatively smaller discharge after NOGO instruction preferred to SR (Fig. 9B). The post-instruction activity was found in seven out of eight FSNs. The corresponding characteristics of post-instruction activity was observed in PANs classified as a "complex association" type, the majority of which was "GO, NOGO(SR)" type to which the FSN activity would belong (Fig. 7 in Hori et al., 2009). Although our sample of FSNs was limited, the timing of activity change (e.g., pre- and post-instruction period) and their selectivity (e.g., specificity to action–reward association) appeared to be comparable between FSNs and PANs in the posterior part of putamen.

The anterior striatum is suggested to be involved in flexible learning of a sequence of action–reward associations. We recorded neuronal activity from the anterior striatum (Fig. 1, green), while one monkey performed a sequential paired-association task (Fig. 3E–G). One example of FSN showed increased discharge after the first cue presentation associated with LR (Fig. 10). Two out of three FSNs showed this type of modulation after the onset of the first cue or the following delay period. Besides, another FSN showed increased activity after no reward during the outcome period (not shown). Comparable reward modulation was found in the majority of PANs showing activities during the first cue presentation and the outcome period, independent of the visual properties of the first cues (Fig. 6 in Pan et al., 2014). FSNs and PANs might therefore encode reward information associated with higher-order conditioned visual stimuli in a similar way.

Collectively, FSNs and PANs seem to encode actions and outcomes similarly during reward-directed hand or eye movements in distinct functional subregions of the striatum. The functional similarity among FSNs and PANs may suggest a common neural substrate of reward-directed actions existed in large parts of the striatum.

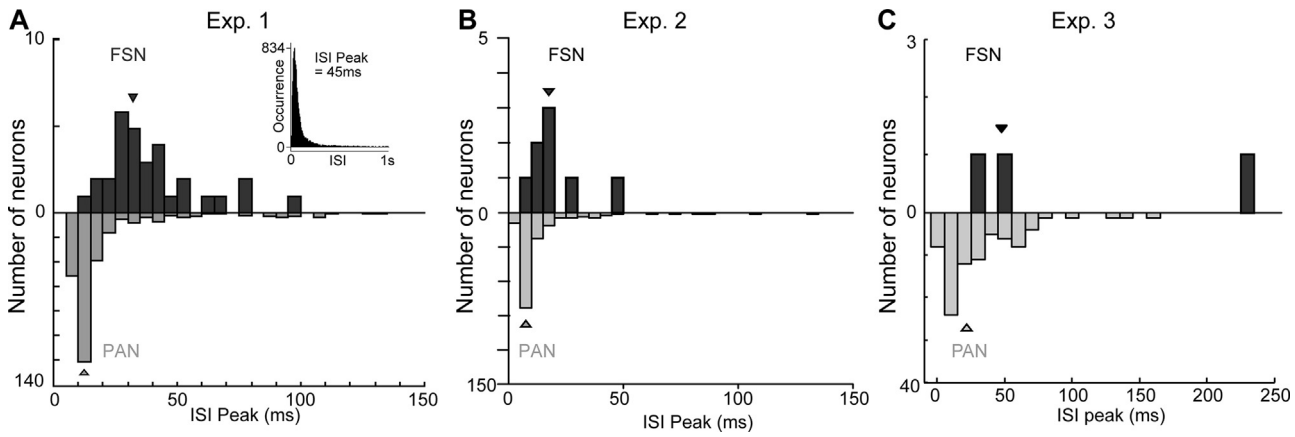

Fig. 7. Temporal activity pattern of FSNs and PANs. (A)–(C) Histograms showing ISI peaks for individual neurons in FSNs (black, upper) and PANs (gray, lower) in experiments 1–3, respectively. Inset in A indicates an example of the ISI distribution and its ISI peak for an example FSN. Triangles indicate median.

3.4. Higher discharge selectivity for actions and outcomes in PANs compared to FSNs

As described above, two classes of striatal neurons similarly encode critical variables in reward-directed behaviors (Fig. 8D). If FSNs contribute to organize striatal output, discharge selectivity for the variables would be higher in PANs than FSNs. To test this possibility, we compared the effect of actions (i.e., target choices) and outcomes (i.e., outcome feedback) on the activities of two neuronal types in experiment 1 quantified by the standardized regression coefficients. The values for both variables were significantly higher in PANs than FSNs (two-way ANOVA, neuron type × variables; neuron type, $P = 0.02$), while the values for outcome feedback were higher than those for the target choices (variables, $P < 0.001$; interaction, $P = 0.47$, Fig. 11). This suggests that the discharge selectivity for both variables was higher in PANs than FSNs.

4. Discussion

In the present study, we analyzed the activity of striatal neurons collected from independent neurophysiological laboratories during reward-directed hand or eye movements in distinct

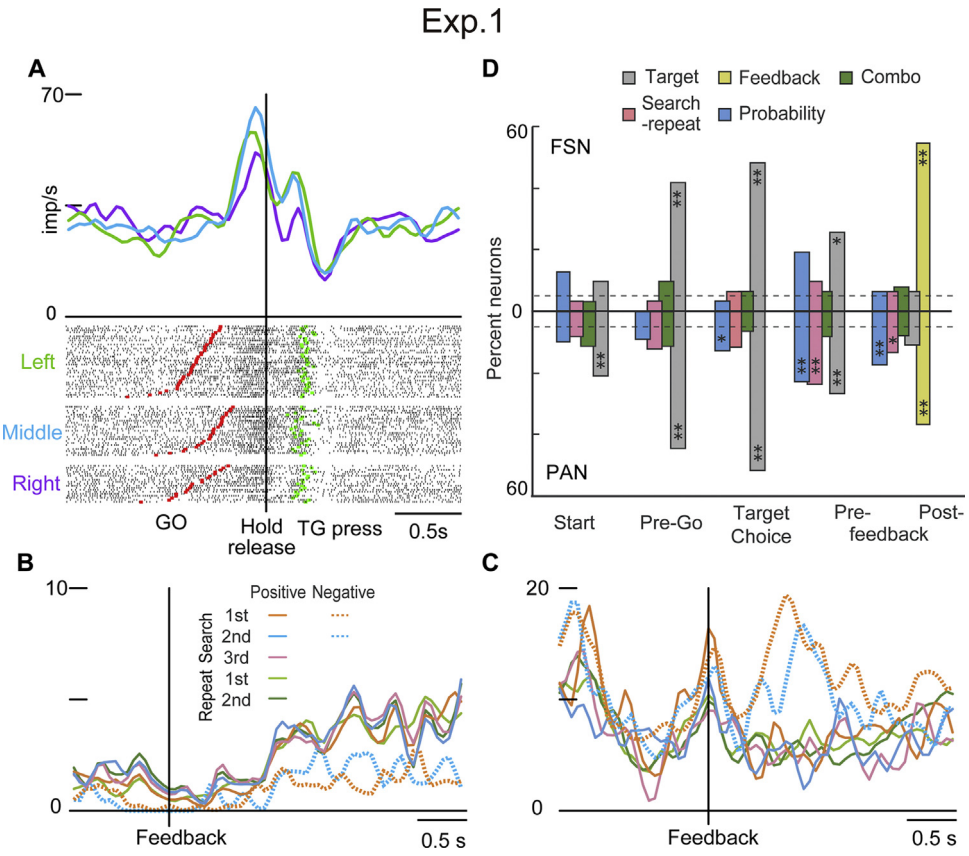

Fig. 8. FSNs encoding target choices and outcome feedback in multistep choice task. (A) An example activity of target-type FSNs. Rasters and histograms were aligned at hold button release for each target that the monkey chose. Red and green marks in the raster indicate GO and target button press, respectively. (B) and (C) Examples of feedback-type FSN activity. The FSNs encode positive (B) and negative (C) outcome feedback, respectively. Histograms (40-ms bins) are smoothed with a Gaussian kernel (40 ms). (D) Histograms showing the percentage of modulation types in FSNs and PANs categorized by multiple regression analysis in each task period. ** and *: statistical significance at $P < 0.01$ and $P < 0.05$ from 5% chance (dashed line) using binominal test.

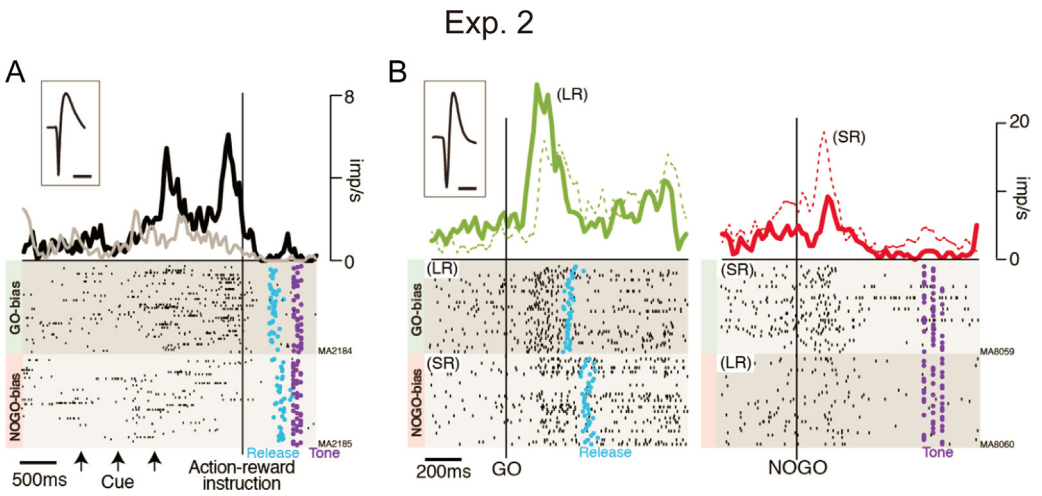

Fig. 9. Activity of FSNs during an asymmetrically rewarded GO-NOGO button-press task. (A) An example activity of FSNs during pre-instruction period differentiated between reward biases. Raster plots show spikes aligned with the action–reward instructions in the chronological order of the trials, separately for GO- and NOGO-bias blocks. Spike density histograms at the top, smoothed with a Gaussian kernel (30 ms), show changes in firing rate in GO-bias blocks (black) and NOGO-bias blocks (gray). (B) An example activity of FSNs during post-instruction period with specificity to action–reward association. Rasters and histograms are aligned at the time of the GO (left, green histograms) or NOGO (right, red histograms) instruction. The format of the diagram is the same as in A. In A and B, the scale bar in the inset indicates 1 ms. (For interpretation of the references to color in this figure legend, the reader is referred to the web version of this article.)

functional subregions of the striatum. We differentiated FSNs from other neurons based on their spike shapes in each experiment. The classification method used in the present study allowed us to integrate multiple small sets of FSN samples into a single group data. Thereafter, we found two properties inherent to FSNs in comparison with PANs. First, temporal profiles of the FSN activity were distinct from those of PANs. FSNs were characterized by their high-frequency regular firings with gradual activity changes in contrast to bursty phasic firings of PANs. The FSN activity continued across several task periods, while the PAN activity occurred only in a few task periods. Second, neural representation of critical variables in reward-directed behaviors was similar but quantitatively different between two classes; while FSNs encoded actions and outcomes in their discharge rates similar to PANs in terms of proportion of neurons, signals carried by PANs were more selective to actions and outcomes than those of FSNs. These characteristics of FSNs were consistent among large parts of the striatum. These findings suggest the possibility that the inhibitory effect of FSNs on PANs

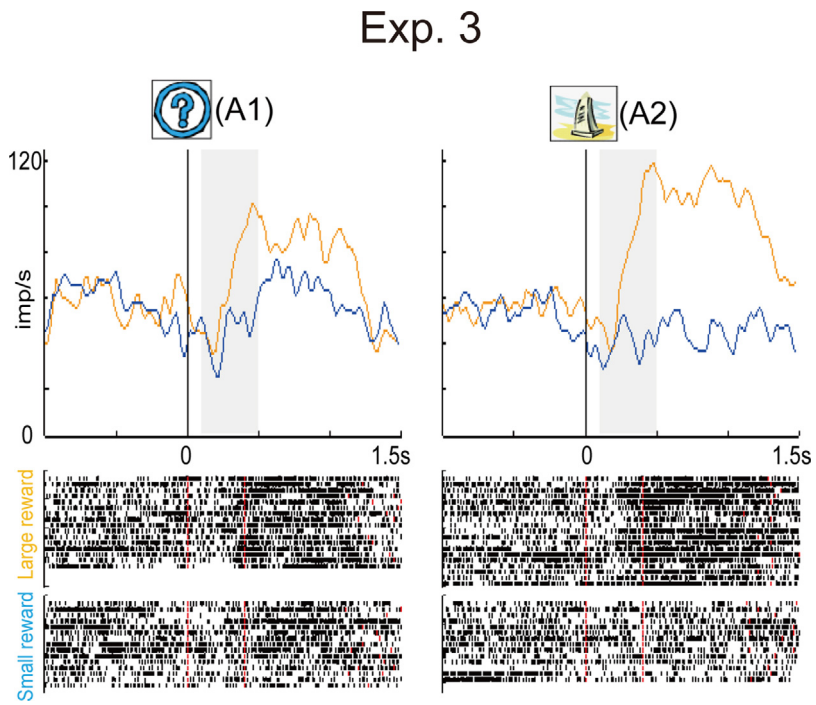

Fig. 10. Activity of FSNs during the performance of sequential paired-association task. An example activity of FSNs under four experimental conditions: the first cue stimuli (A1-left panel, A2-right panel) and the two reward conditions (large reward and small reward). The activity was aligned with the first cue onset. The gray area indicates the period used for analysis of neuronal activity. Neuronal activity was compared between the two reward conditions for each stimulus separately in this time window (two-tailed *t*-test, $P < 0.01$).

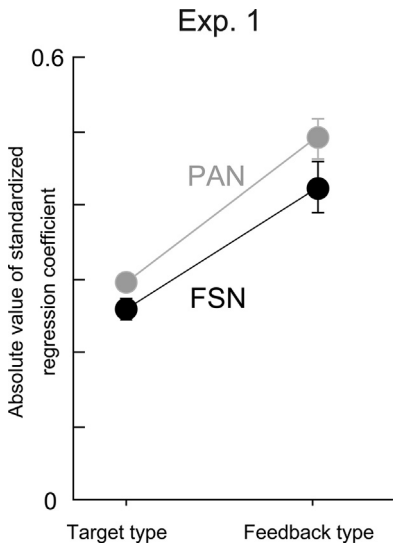

Fig. 11. Coding of target choices and outcome feedback in FSNs and PANs. Absolute value of the standardized regression coefficient of the target choice (target type) and the outcome feedback (feedback type) in the activity of FSNs and PANs. Error bars indicate S.E.

enhances temporal precision and selectivity of the striatal outputs in reward-directed behaviors.

4.1. Identification of FSNs with the spike shape/pattern in vivo primate striatum

In the striatum of behaving monkeys, two major classes of neurons have been identified based on the extracellularly recorded spike shape and firing rates/patterns: PANs and TANs (Aosaki et al., 1994b; DeLong et al., 1986; Hikosaka et al., 1989; Kimura et al., 1990; Morris et al., 2004; Ravel et al., 2003; Romo et al., 1992; Yamada et al., 2004). In rodent striatum, two corresponding classes of neurons in slice preparation are also electrophysiologically classified, and can be identified morphologically and histochemically (Kawaguchi et al., 1995; Wilson, 1995). One class is GABAergic medium spiny projection neurons labeled with substance P/enkephalin in addition to GABA. They constitute the majority (over 90%) of the striatal neurons. Resting potentials of rodent striatal projection neurons in vitro are hyperpolarized far from the action potential threshold (Jiang and North, 1991). They are usually silent in in vivo anesthetized rats and sometimes fire phasically in response to massive input from the cortex (Wilson, 1995). The other class comprises the cholinergic interneurons. They are giant aspiny interneurons labeled with choline acetyltransferase. They show an irregular tonic firing pattern with an average rate of 2–10 Hz in in vivo anesthetized rats (Wilson et al., 1990). These tonic firing properties are due to a unique combination of the electrophysiological properties in rat slice preparation: a prolonged spike afterhyperpolarization and a hyperpolarization-activated cation current (Kawaguchi et al., 1995). A juxtacellular recording study demonstrated that in vivo electrophysiological properties of medium size projection neurons and cholinergic interneurons in anesthetized rats were similar to those of PANs and TANs in behaving monkeys, respectively (Inokawa et al., 2010). These electrophysiological, morphological, and neurochemical properties are recognized as similar between primates and rodents, and it is generally agreed that PANs and TANs recorded from behaving monkeys are the medium spiny projection neurons and cholinergic interneurons, respectively.

In addition to PANs and TANs, FSNs are the third class of neurons classified in the striatum of behaving rodents and have not been fully identified in the striatum of behaving monkeys (although reported by Adler et al., 2013). Recently, several studies classified FSNs in the striatum of behaving rodents (Gage et al., 2010; Lansink et al., 2010; Schmitzer-Torbert and Redish, 2008); the activity of FSNs was electrophysiologically characterized with narrow spike shapes and high-frequency firings compared to other striatal neurons. These electrophysiological properties are consistent with those of the parvalbumin-containing GABAergic interneurons in slice preparation characterized as aspiny, labeled with GABA, but not with substance P/enkephalin. During whole-cell current clamp recording, depolarizing current pulses elicited a series of action potentials with short duration followed by brief afterhyperpolarizations at constant rates (Kawaguchi, 1993). Firing rates of these neurons increased up to 300 Hz with little firing adaptation during strong depolarizing current pulses (Koos and Tepper, 1999; Tepper et al., 2010), and the width of the action potentials was significantly narrower than those of the other interneurons and medium spiny projection neurons (Kawaguchi, 1993; Plotkin et al., 2005). These electrophysiological properties, therefore, permit us to classify the parvalbumin-containing GABAergic interneurons as FSNs in the striatum of behaving primates as well those behaving rodents.

In the present study, we identified FSNs solely based on spike shape as in previous rodent studies in the striatum and cortex (Bartho et al., 2004; Gage et al., 2010). The identified FSNs showed gradual changes in discharge rates compared to the PANs for some task events (Fig. 6). Besides, FSNs exhibited higher discharge rates during task (about 10 Hz) as compared to PANs (Fig. 5) consistent with slice preparation (Kawaguchi, 1993; Koos and Tepper, 1999; Plotkin et al., 2005; Tepper et al., 2010). The average firing rate of FSNs in this study was, however, lower than that of rat FSNs during the performance of choice tasks (about 18 Hz) (Gage et al., 2010). This discrepancy may arise from differences in behavior during instrumental performance as monkeys sat on a chair with restricted body movements, whereas rats restlessly moved around in the experimental chamber. The difference in freedom of body movements might be the cause of the difference in the net effect of the activation of the striatal circuit driven by the cortical and thalamic inputs.

The spike waveform-based classification seemed to provide better performance. In three out of four experiments, two clusters of neurons were clearly separated (Fig. 2). The classification was performed separately for each individual experiment, since spike shapes are strongly dependent on amplifier filter settings: the frequency of low-pass and high-pass filter, and the type of filter (e.g., Butterworth, Bessel, or Chebyshev) (Mizuhiki et al., 2012). This is reassuring because using the same filter and settings (Exps. 1 and 2; band pass, 50 Hz to 3 kHz, Nihonkoden AB-611J) resulted in the separation of clusters at similar spike shape parameters (width at the half max of the negative peak amplitude, 0.28 ms, peak-to-valley width, 0.60 ms; Fig. 2A and B). Compared to spikes in these two experiments, the overall spike widths were narrower in experiments 3 and 4 (Fig. 2C and D) where a band pass was used at high cutoff frequency for high-pass filter (band pass: Exp. 3, 100 Hz to 8 kHz; Exp. 4, 150 Hz to 3 kHz). Especially, in experiment 4, the overlap of the two clusters may have resulted from high-pass filtering at high cutoff frequency which yields narrower spike waveforms (Mizuhiki et al., 2012). In future studies, a lower cut-off frequency for filtering (e.g., 50 Hz to 3 kHz) would be recommended for better differentiation of FSNs from other neurons. It also may be better to use a wide-band filter settings during data acquisition and apply additional filters later.

In summary, we classified three types of neurons in the striatum of behaving monkeys based on spike shape: PANs (presumed projection neurons), TANs (presumed cholinergic interneurons),

and FSNs (presumed parvalbumin-containing GABAergic interneurons). Filtering at low cutoff frequency is suitable for identifying these neuronal types.

4.2. Models of organizing striatal outputs by FSNs

Striatum is the primary input stage of the basal ganglia receiving glutamatergic afferents from the cortex and thalamus, while its outputs are under the control of local GABAergic inhibition (Tepper et al., 2004). Fig. 12A shows a schematic drawing of two types of inhibition to the outputs of striatum, that is, the activity of projection neurons or PANs. It has been shown that parvalbumin-containing GABAergic interneurons have perisomatic synapses with a powerful inhibitory influence on medium spiny projection neurons in rat slice preparation (Koos and Tepper, 1999). This strong suppression of FSNs affects the spike timings or spike generation of PANs (i.e., striatal outputs) driven by cortical and thalamic excitatory inputs (Ramanathan et al., 2002; Rudkin and Sadikot, 1999; Sidibe and Smith, 1999). This is referred to as *feedforward inhibition* (Tepper et al., 2008) and supported by evidence in anesthetized rat striatum (Mallet et al., 2005). The other inhibitory regulation on striatal outputs is *feedback inhibition* that leads to recurrent local inhibition (Fig. 12A). An in vitro rat study showed that neighboring PANs are weakly connected to each other, and the collateral inhibitions are too weak to suppress the neighboring PANs (Tepper et al., 2004). Thus, the feedforward inhibition of FSNs would lead to a powerful control of network outputs in the striatum.

How does the feedforward inhibition control the striatal outputs in behaving animals? We observed that while FSNs showed tonic discharges (Fig. 4), 50% of FSNs showed increased discharge rates at behavioral events and 25% of FSNs showed a decreased discharge rates (Fig. 6C). These observations led us to two possible mechanisms of FSNs controlling PAN discharges, the *Extra-inhibition model* and the *Disinhibition model* (Fig. 12B), for organizing striatal outputs.

Extra-inhibition model: While tonic discharges of FSNs are constantly inhibiting PANs, facilitation of FSN discharges to behavioral events leads to increased inhibitory effect on striatal output neurons (Fig. 12B, left). Under this condition, the phasic activity of PANs would be elicited only if they receive strong coincident inputs to overcome this competitive inhibition. In fact, FSNs showed broadly synchronized firing compared to PANs, and the activity of FSNs preceded that of PANs (Adler et al., 2013), suggesting that common excitatory inputs drive neighboring FSNs and PANs simultaneously. Thus, in addition to constant inhibition, extra-inhibitory inputs from FSNs hyperpolarize the membrane potential of PANs to prevent their firing. This additional inhibitory effect on the output neurons is well suited to suppress PAN discharges following all excitatory inputs but the most optimal ones, leading to improved selectivity of the PANs.

Our results showing facilitation of response in a majority of FSNs (cf. Fig. 6) suggest that extra-inhibition contributes to organizing striatal output. Several lines of circumstantial evidence support the model. First, as observed in this study, PANs exhibit phasic activity for a limited number of task events. This has been commonly observed under various behavioral contexts such as arm movement (Kimura et al., 1990), sequential saccadic and arm movements (Kermadi and Joseph, 1995), memory retrieval of sequential movements (Miyachi et al., 2002; Ueda and Kimura, 2003), and saccades with asymmetric rewards (Kawagoe et al., 1998). Second, in addition to selective activation to specific task events, the phasic activity of PANs occurred within short time periods (half-peak width, 1.23 s; Fig. 6B). This result would support the extra-inhibition model since strong inhibition to PANs might reduce the duration of phasic activity. Competition among the cortical excitatory inputs and local inhibition via FSNs might lead to phasic burst firing of PANs in more restricted behavioral events within a shorter time period. Third, response selectivity for actions and outcomes was higher in PANs than FSNs (Fig. 11), suggesting the enhanced selectivity by inhibition from FSNs to PANs. Thus, our data suggest that extra-inhibition is a neural substrate for controlling the striatal outputs.

Disinhibition model: Given the tonic inhibition of FSNs to PANs, phasic decrease of FSN discharges to behavioral events leads to phasic activation of PANs (Fig. 12B, right). Indeed, we observed a strong decrease of FSN discharges during target choice (Fig. 4B). Suppression response in a fraction of FSNs suggested that some activities of PANs were controlled by disinhibition for gating striatal outputs.

One limitation of our study is that we did not examine the activity of directly connected FSN–PAN pairs. Therefore, we cannot directly test these two models neuron by neuron, but can do so at the population level. Gage et al. suggested that the directional tuning of neighboring FSNs and PANs was opposite in the behaving rodent (Gage et al., 2010). In that study, the activity of FSNs selective to rat choice direction was due to the facilitation and suppression of FSN firing against ipsilateral and contralateral choice, respectively (Fig. 6B in Gage et al., 2010). This bidirectional change of firings at one behavioral event (combination of facilitation and suppression) was not observed in our experiments. Most FSN firings changed to unidirectional for one behavioral event (either facilitation or suppression, Fig. 8–10). This discrepancy suggests that the control mechanisms of animals' choices by striatal FSNs might be somewhat different among these species. Further study is required to elucidate the heterogeneity of FSN function in the striatal local circuit.

4.3. Coordinated coding of actions and outcomes by FSNs and PANs

An unambiguous finding in this study is the coding of actions and outcomes by FSNs in the striatum. Previous rat studies have already indicated that the activity of FSNs is selective to chosen actions in the dorsal striatum (Gage et al., 2010) and reward outcomes in ventral striatum (Lansink et al., 2010). Our results in monkey striatum extended and generalized these individual conclusions in a large part of the striatum. Moreover, our results demonstrated a functional similarity between FSNs and PANs in encoding actions and outcomes, in terms of proportion of neurons (Fig. 8D), despite the finding that the discharge selectivity in encoding actions and outcomes was higher in PANs than FSNs (Fig. 11).

What is the functional significance of the coordinated coding of actions and outcomes that produces such a similarity and difference between FSNs and PANs? As discussed above, if common inputs excite neighboring FSNs and PANs simultaneously in the striatal local circuit, then the coding of actions and outcomes would be similar. Neighboring PANs must be suppressed by the feedforward inhibition, and threshold to elicit phasic activation of PANs must increase (as proposed by the extra-inhibition model). On the contrary, if divergent inputs drive these adjacent striatal neurons, both FSNs and PANs might sometimes encode actions and outcomes, but the selectivity of the discharge could be opposite due to feedforward inhibition as observed by Gage et al. (2010). Balance of the feedback and feedforward inhibition as a function of tonic as well as phasic components of discharges seems to be involved in organizing striatal outputs. Further study is required to elucidate the local circuit dynamics as input–output structures produced by local inhibition in the striatum.

4.4. Comparison with organizing striatal outputs via TANs

The role of the striatal interneurons known as TANs has been well examined during reward-directed behaviors in monkeys. TANs

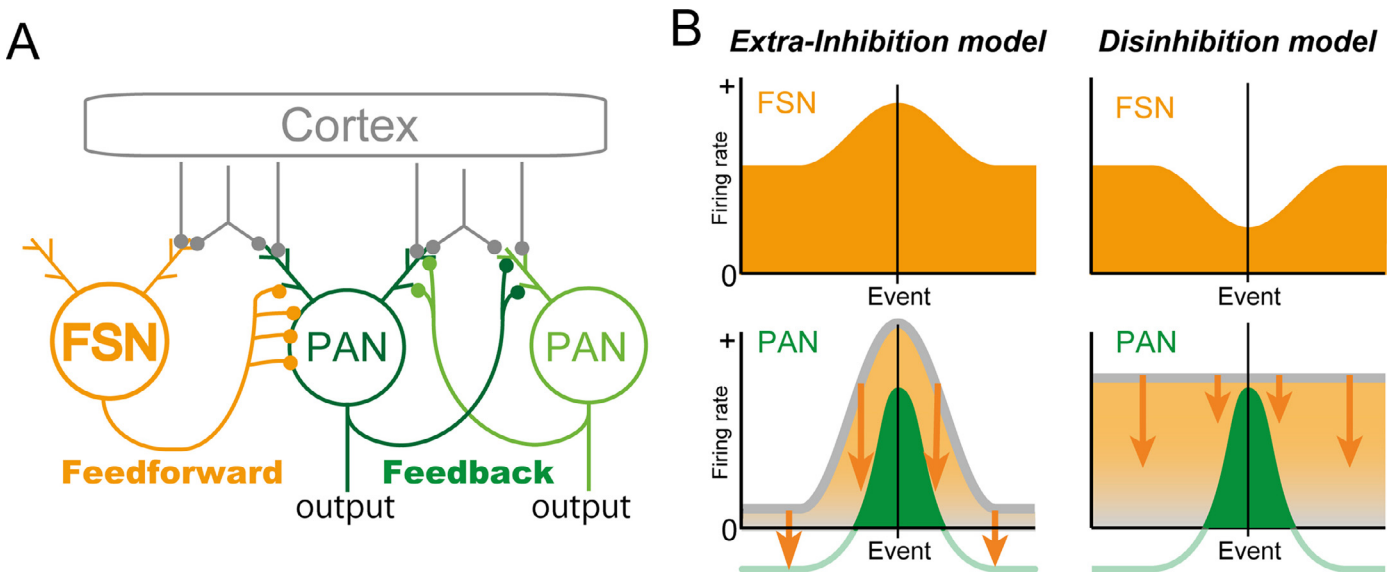

Fig. 12. Diagram of FSN function in controlling PAN discharges during monkey behavior. (A) Schematic drawing of the FSN–PAN and PAN–PAN connections in the striatum (modified Tepper et al., 2004). (B) Schematic drawing of two alternative functional models of FSN. In extra-inhibition model (left), increase of FSN discharges at around a task event (orange) suppresses the coincident activation of PAN (gray) that is driven by event-related excitatory inputs (gray). Thus, PAN responds more phasically to the event (green). In the disinhibition model (right), decreased discharges of FSN around an event (orange) lead to the activation of PAN (green) even without event-related excitatory inputs (gray). (For interpretation of the references to color in this figure legend, the reader is referred to the web version of this article.)

showed irregular tonic firing at about 2–8 Hz. During classical and instrumental conditioning, they showed brief pauses in tonic firing followed by a transient increase of the discharge in response to rewarding cues (Apicella et al., 1991; Kimura, 1990; Kimura et al., 1984). These characteristic responses of TANs were differentially observed neuron by neuron when rewarding and aversive cues drive the monkeys' behavior (Joshua et al., 2008; Ravel et al., 2003; Yamada et al., 2004). Acetylcholine is one of the neuromodulators, which controls synaptic plasticity in the striatum (Calabresi et al., 2000). Hence, TANs showed lack of direct facilitation or suppression effect on PAN firing (Adler et al., 2013), but play a role as a learning signal which collaborates with the dopamine signal in the striatum (Aosaki et al., 1994a; Calabresi and Di Filippo, 2008; Morris et al., 2004). TANs modulate activity of various classes of striatal neurons: PANs, TANs, and FSNs as well as dopamine release from its terminal (Calabresi et al., 2000; Cragg, 2006; Koos and Tepper, 2002). Thus, modulatory signal of TANs may exert some control over the activity of the striatal local circuit.

4.5. Activity of FSNs and cortico-basal ganglia loop

Striatum is composed of distinct functional subregions in view of the input–output structure as suggested by the cortico-basal ganglia loop (Alexander et al., 1986; Haber, 2003). Each functional loop, that is, motor, oculomotor, associative, and limbic loop, plays a distinct role in reward processes (Balleine et al., 2007; Miyachi et al., 1997; Muranishi et al., 2011; Nakamura and Hikosaka, 2006; O'Doherty et al., 2004; Williams and Eskandar, 2006). Our samples from various striatal subregions reveal the coordinated coding of actions and outcomes by FSNs and PANs.

The motor striatum receives inputs from motor cortices such as primary motor cortex, pre-motor cortex, and the supplementary motor area (Nambu et al., 2002; Takada et al., 2001), and send back the output to the motor cortices via the internal segment of the globus pallidus/substantia nigra pars reticulata and thalamus for limb movements. The oculomotor striatum, such as caudate nucleus, mainly receives inputs from the frontal eye field and the supplemental eye field to control eye movement (Hikosaka et al., 2000). It has been demonstrated that PANs in the motor and oculomotor striatum play a role in controlling hand and eye movements toward rewarding targets, respectively (Hori et al., 2009; Kawagoe et al., 1998; Kermadi and Joseph, 1995; Nakamura and Hikosaka, 2006; Pasquereau et al., 2007; Samejima et al., 2005). Consistent with those findings, FSNs in the motor striatum (i.e., the posterior part of the putamen) showed activity in guiding monkeys' actions toward rewards (Exp. 2). It was shown that FSNs as well as PANs in the putamen also similarly responded to rewarding and aversive cues during classical conditioning (Adler et al., 2013). Moreover, FSNs in the caudate nucleus and putamen similarly encoded actions and outcomes during value-based decision-making (Exp. 1). Thus, FSNs in the distinct subregions of the striatum seemed to be involved in guiding actions toward rewards.

Another functional subregion of the striatum, the anterior striatum, was suggested to guide animal's actions toward rewards by quickly adjusting action–outcome associations through learning in monkeys (Pasupathy and Miller, 2005; Williams and Eskandar, 2006). In line with this view, we found that FSNs in the anterior striatum adaptively encoded reward-associated actions in the sequential paired-association task (Exp. 3). Indeed, we recorded the activity of FSNs and PANs in a large part of the striatum under various task contexts. FSNs and PANs showed considerable similarity in their discharges in encoding actions and outcomes (Figs. 8–10), while they represented the crucial information for guiding actions toward outcomes in each task context, depending on the inputs in each subregion of the striatum.

What signals are involved in establishing the coordinated activity of FSNs and PANs in distinct functional subregions of the striatum? Striatal neurons, FSNs, PANs, and TANs, are under the control of two learning signals, dopamine and acetylcholine (Calabresi et al., 2000; Calabresi and Di Filippo, 2008; Calabresi et al., 2007; Pisani et al., 2007; Surmeier et al., 2011; Tritsch and Sabatini, 2012). Midbrain dopamine neurons send a signal of reward prediction error to the striatum (Houk et al., 1995; Montague et al., 1996; Schultz et al., 1997), and they also signal saliency, novelty, and motivation level for adaptive learning (Matsumoto and Hikosaka, 2009; Satoh et al., 2003; Zald et al.,

2008). Coincident cholinergic signals with dopaminergic signals in the striatum encode rewarding and aversive motivational outcomes (Joshua et al., 2008; Ravel et al., 2003; Yamada et al., 2004), and individual cholinergic interneurons govern the local striatal circuits. The cholinergic signals are more heterogeneous neuron by neuron (Yamada et al., 2004) as compared to the dopaminergic signals, suggesting that the activity of FSNs and PANs would be distinctive neuron by neuron, but cooperative in each local circuit. These characteristics of the striatal local circuit could underlie adaptive learning through the cortico-basal ganglia circuit, during which subjects explore various behavioral environments depending on their internal motivational state (Dickinson and Balleine, 1994; Minamimoto et al., 2009; Yamada et al., 2013b).

4.6. Comparison with FSNs in cerebral cortex

Our data suggest that FSNs modulate striatal output while enhancing discharge selectivity. Similar modulation by inhibitory interneurons is also suggested in cerebral cortex. FSNs labeled by parvalbumin immunoreactivity in the area V1 of mice are shown to be selectively involved in shaping orientation tuning and enhancement of directional selectivity of the neighboring neurons (Lee et al., 2012). In addition, the inhibitory role of FSNs has been suggested to improve various cognitive functions in distinct cortical regions. For example, FSNs in monkey prefrontal cortex demonstrated their relation to the learning and performance of cognitive tasks (Constantinidis and Goldman-Rakic, 2002; Qi and Constantinidis, 2012). FSNs in the visual area V4 showed their modulation in their control of attention (Mitchell et al., 2007), suggesting that reliability of output neuron response is increased by reducing response variability. Thus, the feedforward inhibition could be a general mechanism for improving output selectivity, though the input structure is the key factor in driving a local network.

4.7. Dysfunction of the striatal local circuit and cortico-basal ganglia loop

Dysfunction of FSNs may underlie a key pathophysiology of Tourette syndrome (TS), a chronic neuropsychiatric disorder characterized by motor and phonic tics. Decrement in parvalbumin-containing GABAergic interneurons has been evident in TS patients (Kalanithi et al., 2005; Kataoka et al., 2010). Focal disruption of GABAergic network in the striatum via injection of $GABA_A$ antagonist elicits tic-like movements in monkeys. In this model, different types of abnormal movements are observed depending on the location of inhibitory dysfunction with regard to the striatal functional subregions; motor tics are induced via sensorimotor circuits, whereas dysfunction in limbic loop induces complex tics containing vocal tics and some facial expressions (Crossman et al., 1984; McCairn et al., 2009, 2013; Worbe et al., 2009). It is hypothesized that tics arise from the aberrant activation of a small population of PANs that correspond to specific motor commands (Albin and Mink, 2006). This is consistent with the disinhibition model described above (Fig. 12B, right) which suggests that the focal attenuation of the constant inhibition may excite a subset of striatal neurons encoding distinct actions leading to repetitive inappropriate movements.

FSNs may also contribute to symptoms of Parkinson's disease (PD), caused by dopamine neuronal degeneration. While alternative deregulations of striatal outputs via direct and indirect pathways constitute the main functional pathology of PD (Gerfen et al., 1990; Gerfen and Surmeier, 2011; Gertler et al., 2008), FSNs may have an additional role in shaping the functional properties of these pathways (Gittis et al., 2011; Mallet et al., 2006). Imbalance of these striatal outputs derived from the changes of GABAergic connectivity may result in abnormal activity in the downstream circuit (Ballion et al., 2008; Cruz et al., 2009, 2011; Mallet et al., 2012).

Thus, dopamine-dependent and dopamine-independent deficits of the cognitive and motor skills could emerge from the dysfunction of FSNs themselves and the adjacent local circuits through the cortico-basal ganglia loop. Inhibition maintained by two distinct ways (Fig. 12B) may be unbalanced in the striatal local circuit, and these symptoms may evolve throughout cortico-basal ganglia functional loops.

4.8. Conclusions

We studied striatal neuron activity in behaving monkeys collected from independent neurophysiological laboratories. Spike waveform analysis provides a reliable means for identifying FSNs and allows quantitative assessments of integrated datasets. Similarity and dissimilarity of the characteristic activity between FSNs and PANs were evident in their basic firings and discharge selectivity during reward-directed behaviors. Based on these findings, we propose two feedforward inhibition models of FSNs to control activity of PANs. The integrated multiple sets of data further suggest that these feedforward controls are implemented across striatal subregions to enhance tuning of striatal outputs. Overall, our results provide a valuable platform for future challenges including (1) understanding the striatal mechanisms of reward-directed behavior in nonhuman primates, (2) translating the findings of neurophysiological studies in rodents, and (3) elucidating the pathophysiological mechanisms underlying symptoms of brain disorders, such as TS and PD.

Acknowledgments

The authors wish to express their appreciation to M. Matsumoto and K. Seki. This research was supported by the Grant-in-Aid for Scientific Research on Priority Areas from the Ministry of Education, Culture, Sports, Science, and Technology, MEXT Japan (H.Y.: 15H05374, Y.H.: NO20900293) and by the Grant-in-Aid for Scientific Research on Innovative Areas from the Ministry of Education, Culture, Sports, Science, and Technology, MEXT Japan (M.S.: 23120001). X.P. is supported by National Natural Science Foundation of China (No. 11232005) and Shanghai Pujiang Program (13PJ1402000).

References

Adler, A., Katabi, S., Finkes, I., Prut, Y., Bergman, H., 2013. Different correlation patterns of cholinergic and GABAergic interneurons with striatal projection neurons. Front. Syst. Neurosci. 7, 47.

Albin, R.L., Mink, J.W., 2006. Recent advances in Tourette syndrome research. Trends Neurosci. 29 (3), 175–182.

Alexander, G.E., DeLong, M.R., Strick, P.L., 1986. Parallel organization of functionally segregated circuits linking basal ganglia and cortex. Annu. Rev. Neurosci. 9, 357–381.

Aosaki, T., Graybiel, A.M., Kimura, M., 1994a. Effect of the nigrostriatal dopamine system on acquired neural responses in the striatum of behaving monkeys. Science 265 (5170), 412–415.

Aosaki, T., Tsubokawa, H., Ishida, A., Watanabe, K., Graybiel, A.M., Kimura, M., 1994b. Responses of tonically active neurons in the primate's striatum undergo systematic changes during behavioral sensorimotor conditioning. J. Neurosci. 14 (6), 3969–3984.

Apicella, P., Scarnati, E., Schultz, W., 1991. Tonically discharging neurons of monkey striatum respond to preparatory and rewarding stimuli. Exp. Brain Res. 84 (3), 672–675.

Balleine, B.W., Delgado, M.R., Hikosaka, O., 2007. The role of the dorsal striatum in reward and decision-making. J. Neurosci. 27 (31), 8161–8165.

Ballion, B., Mallet, N., Bezard, E., Lanciego, J.L., Gonon, F., 2008. Intratelencephalic corticostriatal neurons equally excite striatonigral and striatopallidal neurons and their discharge activity is selectively reduced in experimental parkinsonism. Eur. J. Neurosci. 27 (9), 2313–2321.

Bartho, P., Hirase, H., Monconduit, L., Zugaro, M., Harris, K.D., Buzsaki, G., 2004. Characterization of neocortical principal cells and interneurons by network interactions and extracellular features. J. Neurophysiol. 92 (1), 600–608.

Cai, X., Kim, S., Lee, D., 2011. Heterogeneous coding of temporally discounted values in the dorsal and ventral striatum during intertemporal choice. Neuron 69 (1), 170–182.
Calabresi, P., Centonze, D., Gubellini, P., Pisani, A., Bernardi, G., 2000. Acetylcholine-mediated modulation of striatal function. Trends Neurosci. 23 (3), 120–126.
Calabresi, P., Di Filippo, M., 2008. ACh/dopamine crosstalk in motor control and reward: a crucial role for alpha 6-containing nicotinic receptors? Neuron 60 (1), 4–7.
Calabresi, P., Picconi, B., Tozzi, A., Di Filippo, M., 2007. Dopamine-mediated regulation of corticostriatal synaptic plasticity. Trends Neurosci. 30 (5), 211–219.
Constantinidis, C., Goldman-Rakic, P.S., 2002. Correlated discharges among putative pyramidal neurons and interneurons in the primate prefrontal cortex. J. Neurophysiol. 88 (6), 3487–3497.
Cragg, S.J., 2006. Meaningful silences: how dopamine listens to the ACh pause. Trends Neurosci. 29 (3), 125–131.
Crossman, A.R., Sambrook, M.A., Jackson, A., 1984. Experimental hemichorea/hemiballismus in the monkey. Studies on the intracerebral site of action in a drug-induced dyskinesia. Brain 107 (Pt 2), 579–596.
Cruz, A.V., Mallet, N., Magill, P.J., Brown, P., Averbeck, B.B., 2009. Effects of dopamine depletion on network entropy in the external globus pallidus. J. Neurophysiol. 102 (2), 1092–1102.
Cruz, A.V., Mallet, N., Magill, P.J., Brown, P., Averbeck, B.B., 2011. Effects of dopamine depletion on information flow between the subthalamic nucleus and external globus pallidus. J. Neurophysiol. 106 (4), 2012–2023.
DeLong, M.R., Alexander, G.E., Mitchell, S.J., Richardson, R.T., 1986. The contribution of basal ganglia to limb control. Prog. Brain Res. 64, 161–174.
Dickinson, A., Balleine, B., 1994. Motivational control of goal-directed action. Anim. Learn. Behav. 22, 1–18.
Gage, G.J., Stoetzner, C.R., Wiltschko, A.B., Berke, J.D., 2010. Selective activation of striatal fast-spiking interneurons during choice execution. Neuron 67 (3), 466–479.
Garenne, A., Pasquereau, B., Guthrie, M., Bioulac, B., Boraud, T., 2011. Basal Ganglia preferentially encode context dependent choice in a two-armed bandit task. Front. Syst. Neurosci. 5, 23.
Gerfen, C.R., Engber, T.M., Mahan, L.C., Susel, Z., Chase, T.N., Monsma Jr., F.J., Sibley, D.R., 1990. D1 and D2 dopamine receptor-regulated gene expression of striatonigral and striatopallidal neurons. Science 250 (4986), 1429–1432.
Gerfen, C.R., Surmeier, D.J., 2011. Modulation of striatal projection systems by dopamine. Annu. Rev. Neurosci. 34, 441–466.
Gertler, T.S., Chan, C.S., Surmeier, D.J., 2008. Dichotomous anatomical properties of adult striatal medium spiny neurons. J. Neurosci. 28 (43), 10814–10824.
Gittis, A.H., Hang, G.B., LaDow, E.S., Shoenfeld, L.R., Atallah, B.V., Finkbeiner, S., Kreitzer, A.C., 2011. Rapid target-specific remodeling of fast-spiking inhibitory circuits after loss of dopamine. Neuron 71 (5), 858–868.
Goldberg, J.A., Ding, J.B., Surmeier, D.J., 2012. Muscarinic modulation of striatal function and circuitry. Handb. Exp. Pharmacol. (208), 223–241.
Haber, S.N., 2003. The primate basal ganglia: parallel and integrative networks. J. Chem. Neuroanat. 26 (4), 317–330.
Hikosaka, O., Sakamoto, M., Usui, S., 1989. Functional properties of monkey caudate neurons. I. Activities related to saccadic eye movements. J. Neurophysiol. 61 (4), 780–798.
Hikosaka, O., Takikawa, Y., Kawagoe, R., 2000. Role of the basal ganglia in the control of purposive saccadic eye movements. Physiol. Rev. 80 (3), 953–978.
Hori, Y., Minamimoto, T., Kimura, M., 2009. Neuronal encoding of reward value and direction of actions in the primate putamen. J. Neurophysiol. 102 (6), 3530–3543.
Houk, J.C., Adams, J.L., Barto, A.G., 1995. In: Houk, J.C., Davis, J.L., Beiser, D.G. (Eds.), Models of Information Processing in the Basal Ganglia. The MIT Press, Cambridge, pp. 249–270.
Inokawa, H., Yamada, H., Matsumoto, N., Muranishi, M., Kimura, M., 2010. Juxtacellular labeling of tonically active neurons and phasically active neurons in the rat striatum. Neuroscience 168 (2), 395–404.
Jiang, Z.G., North, R.A., 1991. Membrane properties and synaptic responses of rat striatal neurones in vitro. J. Physiol. 443, 533–553.
Jog, M.S., Kubota, Y., Connolly, C.I., Hillegaart, V., Graybiel, A.M., 1999. Building neural representations of habits. Science 286 (5445), 1745–1749.
Joshua, M., Adler, A., Mitelman, R., Vaadia, E., Bergman, H., 2008. Midbrain dopaminergic neurons and striatal cholinergic interneurons encode the difference between reward and aversive events at different epochs of probabilistic classical conditioning trials. J. Neurosci. 28 (45), 11673–11684.
Kalanithi, P.S., Zheng, W., Kataoka, Y., DiFiglia, M., Grantz, H., Saper, C.B., Schwartz, M.L., Leckman, J.F., Vaccarino, F.M., 2005. Altered parvalbumin-positive neuron distribution in basal ganglia of individuals with Tourette syndrome. Proc. Natl. Acad. Sci. U. S. A. 102 (37), 13307–13312.
Kataoka, Y., Kalanithi, P.S., Grantz, H., Schwartz, M.L., Saper, C., Leckman, J.F., Vaccarino, F.M., 2010. Decreased number of parvalbumin and cholinergic interneurons in the striatum of individuals with Tourette syndrome. J. Comp. Neurol. 518 (3), 277–291.
Kawagoe, R., Takikawa, Y., Hikosaka, O., 1998. Expectation of reward modulates cognitive signals in the basal ganglia. Nat. Neurosci. 1 (5), 411–416.
Kawaguchi, Y., 1993. Physiological, morphological, and histochemical characterization of three classes of interneurons in rat neostriatum. J. Neurosci. 13 (11), 4908–4923.
Kawaguchi, Y., Wilson, C.J., Augood, S.J., Emson, P.C., 1995. Striatal interneurones: chemical, physiological and morphological characterization [published erratum appears in Trends Neurosci 1996 Apr;19(4):143]. Trends Neurosci. 18 (12), 527–535.
Kermadi, I., Joseph, J.P., 1995. Activity in the caudate nucleus of monkey during spatial sequencing. J. Neurophysiol. 74 (3), 911–933.
Kimura, M., 1990. Behaviorally contingent property of movement-related activity of the primate putamen. J. Neurophysiol. 63 (6), 1277–1296.
Kimura, M., Kato, M., Shimazaki, H., 1990. Physiological properties of projection neurons in the monkey striatum to the globus pallidus. Exp. Brain Res. 82 (3), 672–676.
Kimura, M., Rajkowski, J., Evarts, E., 1984. Tonically discharging putamen neurons exhibit set-dependent responses. Proc. Natl. Acad. Sci. U. S. A. 81 (15), 4998–5001.
Koos, T., Tepper, J.M., 1999. Inhibitory control of neostriatal projection neurons by GABAergic interneurons. Nat. Neurosci. 2 (5), 467–472.
Koos, T., Tepper, J.M., 2002. Dual cholinergic control of fast-spiking interneurons in the neostriatum. J. Neurosci. 22 (2), 529–535.
Lansink, C.S., Goltstein, P.M., Lankelma, J.V., Pennartz, C.M., 2010. Fast-spiking interneurons of the rat ventral striatum: temporal coordination of activity with principal cells and responsiveness to reward. Eur. J. Neurosci. 32 (3), 494–508.
Lau, B., Glimcher, P.W., 2008. Value representations in the primate striatum during matching behavior. Neuron 58 (3), 451–463.
Lee, S.H., Kwan, A.C., Zhang, S., Phoumthipphavong, V., Flannery, J.G., Masmanidis, S.C., Taniguchi, H., Huang, Z.J., Zhang, F., Boyden, E.S., Deisseroth, K., Dan, Y., 2012. Activation of specific interneurons improves V1 feature selectivity and visual perception. Nature 488 (7411), 379–383.
Mallet, N., Ballion, B., Le Moine, C., Gonon, F., 2006. Cortical inputs and GABA interneurons imbalance projection neurons in the striatum of parkinsonian rats. J. Neurosci. 26 (14), 3875–3884.
Mallet, N., Le Moine, C., Charpier, S., Gonon, F., 2005. Feedforward inhibition of projection neurons by fast-spiking GABA interneurons in the rat striatum in vivo. J. Neurosci. 25 (15), 3857–3869.
Mallet, N., Micklem, B.R., Henny, P., Brown, M.T., Williams, C., Bolam, J.P., Nakamura, K.C., Magill, P.J., 2012. Dichotomous organization of the external globus pallidus. Neuron 74 (6), 1075–1086.
Matsumoto, M., Hikosaka, O., 2009. Two types of dopamine neuron distinctly convey positive and negative motivational signals. Nature 459 (7248), 837–841.
McCairn, K.W., Bronfeld, M., Belelovsky, K., Bar-Gad, I., 2009. The neurophysiological correlates of motor tics following focal striatal disinhibition. Brain 132 (Pt 8), 2125–2138.
McCairn, K.W., Iriki, A., Isoda, M., 2013. Global dysrhythmia of cerebro-basal ganglia-cerebellar networks underlies motor tics following striatal disinhibition. J. Neurosci. 33 (2), 697–708.
Minamimoto, T., La Camera, G., Richmond, B.J., 2009. Measuring and modeling the interaction among reward size, delay to reward, and satiation level on motivation in monkeys. J. Neurophysiol. 101 (1), 437–447.
Mitchell, J.F., Sundberg, K.A., Reynolds, J.H., 2007. Differential attention-dependent response modulation across cell classes in macaque visual area V4. Neuron 55 (1), 131–141.
Miyachi, S., Hikosaka, O., Lu, X., 2002. Differential activation of monkey striatal neurons in the early and late stages of procedural learning. Exp. Brain Res. 146 (1), 122–126.
Miyachi, S., Hikosaka, O., Miyashita, K., Karadi, Z., Rand, M.K., 1997. Differential roles of monkey striatum in learning of sequential hand movement. Exp. Brain Res. 115 (1), 1–5.
Mizuhiki, T., Inaba, K., Setogawa, T., Toda, K., Ozaki, S., Shidara, M., 2012. The influence of passband limitation on the waveform of extracellular action potential. Neurosci. Res. 72 (3), 214–220.
Montague, P.R., Dayan, P., Sejnowski, T.J., 1996. A framework for mesencephalic dopamine systems based on predictive Hebbian learning. J. Neurosci. 16 (5), 1936–1947.
Morris, G., Arkadir, D., Nevet, A., Vaadia, E., Bergman, H., 2004. Coincident but distinct messages of midbrain dopamine and striatal tonically active neurons. Neuron 43 (1), 133–143.
Muranishi, M., Inokawa, H., Yamada, H., Ueda, Y., Matsumoto, N., Nakagawa, M., Kimura, M., 2011. Inactivation of the putamen selectively impairs reward history-based action selection. Exp. Brain Res. 209 (2), 235–246.
Nakamura, K., Hikosaka, O., 2006. Facilitation of saccadic eye movements by postsaccadic electrical stimulation in the primate caudate. J. Neurosci. 26 (50), 12885–12895.
Nakamura, K., Santos, G.S., Matsuzaki, R., Nakahara, H., 2012. Differential reward coding in the subdivisions of the primate caudate during an oculomotor task. J. Neurosci. 32 (45), 15963–15982.
Nambu, A., Kaneda, K., Tokuno, H., Takada, M., 2002. Organization of corticostriatal motor inputs in monkey putamen. J. Neurophysiol. 88 (4), 1830–1842.
O'Doherty, J., Dayan, P., Schultz, J., Deichmann, R., Friston, K., Dolan, R.J., 2004. Dissociable roles of ventral and dorsal striatum in instrumental conditioning. Science 304 (5669), 452–454.
Pan, X., Fan, H., Sawa, K., Tsuda, I., Tsukada, M., Sakagami, M., 2014. Reward inference by primate prefrontal and striatal neurons. J. Neurosci. 34 (4), 1380–1396.
Pasquereau, B., Nadjar, A., Arkadir, D., Bezard, E., Goillandeau, M., Bioulac, B., Gross, C.E., Boraud, T., 2007. Shaping of motor responses by incentive values through the basal ganglia. J. Neurosci. 27 (5), 1176–1183.
Pasupathy, A., Miller, E.K., 2005. Different time courses of learning-related activity in the prefrontal cortex and striatum. Nature 433 (7028), 873–876.
Pisani, A., Bernardi, G., Ding, J., Surmeier, D.J., 2007. Re-emergence of striatal cholinergic interneurons in movement disorders. Trends Neurosci. 30 (10), 545–553.

Plotkin, J.L., Wu, N., Chesselet, M.F., Levine, M.S., 2005. Functional and molecular development of striatal fast-spiking GABAergic interneurons and their cortical inputs. Eur. J. Neurosci. 22 (5), 1097–1108.
Qi, X.L., Constantinidis, C., 2012. Correlated discharges in the primate prefrontal cortex before and after working memory training. Eur. J. Neurosci. 36 (11), 3538–3548.
Ramanathan, S., Hanley, J.J., Deniau, J.M., Bolam, J.P., 2002. Synaptic convergence of motor and somatosensory cortical afferents onto GABAergic interneurons in the rat striatum. J. Neurosci. 22 (18), 8158–8169.
Ravel, S., Legallet, E., Apicella, P., 2003. Responses of tonically active neurons in the monkey striatum discriminate between motivationally opposing stimuli. J. Neurosci. 23 (24), 8489–8497.
Romo, R., Scarnati, E., Schultz, W., 1992. Role of primate basal ganglia and frontal cortex in the internal generation of movements. II. Movement-related activity in the anterior striatum. Exp. Brain Res. 91 (3), 385–395.
Rudkin, T.M., Sadikot, A.F., 1999. Thalamic input to parvalbumin-immunoreactive GABAergic interneurons: organization in normal striatum and effect of neonatal decortication. Neuroscience 88 (4), 1165–1175.
Samejima, K., Ueda, Y., Doya, K., Kimura, M., 2005. Representation of action-specific reward values in the striatum. Science 310 (5752), 1337–1340.
Satoh, T., Nakai, S., Sato, T., Kimura, M., 2003. Correlated coding of motivation and outcome of decision by dopamine neurons. J. Neurosci. 23 (30), 9913–9923.
Schmitzer-Torbert, N.C., Redish, A.D., 2008. Task-dependent encoding of space and events by striatal neurons is dependent on neural subtype. Neuroscience 153 (2), 349–360.
Schultz, W., Dayan, P., Montague, P.R., 1997. A neural substrate of prediction and reward. Science 275 (5306), 1593–1599.
Schultz, W., Tremblay, L., Hollerman, J.R., 2003. Changes in behavior-related neuronal activity in the striatum during learning. Trends Neurosci. 26 (6), 321–328.
Schulz, J.M., Reynolds, J.N., 2013. Pause and rebound: sensory control of cholinergic signaling in the striatum. Trends Neurosci. 36 (1), 41–50.
Sidibe, M., Smith, Y., 1999. Thalamic inputs to striatal interneurons in monkeys: synaptic organization and co-localization of calcium binding proteins. Neuroscience 89 (4), 1189–1208.
Surmeier, D.J., Carrillo-Reid, L., Bargas, J., 2011. Dopaminergic modulation of striatal neurons, circuits, and assemblies. Neuroscience 198, 3–18.
Takada, M., Tokuno, H., Hamada, I., Inase, M., Ito, Y., Imanishi, M., Hasegawa, N., Akazawa, T., Hatanaka, N., Nambu, A., 2001. Organization of inputs from cingulate motor areas to basal ganglia in macaque monkey. Eur. J. Neurosci. 14 (10), 1633–1650.
Tepper, J.M., Koos, T., Wilson, C.J., 2004. GABAergic microcircuits in the neostriatum. Trends Neurosci. 27 (11), 662–669.
Tepper, J.M., Tecuapetla, F., Koos, T., Ibanez-Sandoval, O., 2010. Heterogeneity and diversity of striatal GABAergic interneurons. Front. Neuroanat. 4, 150.
Tepper, J.M., Wilson, C.J., Koos, T., 2008. Feedforward and feedback inhibition in neostriatal GABAergic spiny neurons. Brain Res. Rev. 58 (2), 272–281.
Tritsch, N.X., Sabatini, B.L., 2012. Dopaminergic modulation of synaptic transmission in cortex and striatum. Neuron 76 (1), 33–50.
Ueda, Y., Kimura, M., 2003. Encoding of direction and combination of movements by primate putamen neurons. Eur. J. Neurosci. 18 (4), 980–994.
Williams, Z.M., Eskandar, E.N., 2006. Selective enhancement of associative learning by microstimulation of the anterior caudate. Nat. Neurosci. 9 (4), 562–568.
Wilson, C.J., 1995. The contribution of cortical neurons to the firing patterns of striatal spiny neurons. In: Models of Information Processing in the Basal Ganglia. MIT Press, Cambridge, pp. 28–50.
Wilson, C.J., 2007. GABAergic inhibition in the neostriatum. Prog. Brain Res. 160, 91–110.
Wilson, C.J., Chang, H.T., Kitai, S.T., 1990. Firing patterns and synaptic potentials of identified giant aspiny interneurons in the rat neostriatum. J. Neurosci. 10 (2), 508–519.
Worbe, Y., Baup, N., Grabli, D., Chaigneau, M., Mounayar, S., McCairn, K., Feger, J., Tremblay, L., 2009. Behavioral and movement disorders induced by local inhibitory dysfunction in primate striatum. Cereb. Cortex 19 (8), 1844–1856.
Yamada, H., Inokawa, H., Matsumoto, N., Ueda, Y., Enomoto, K., Kimura, M., 2013a. Coding of the long-term value of multiple future rewards in the primate striatum. J. Neurophysiol. 109 (4), 1140–1151.
Yamada, H., Inokawa, H., Matsumoto, N., Ueda, Y., Kimura, M., 2011. Neuronal basis for evaluating selected action in the primate striatum. Eur. J. Neurosci. 34 (3), 489–506.
Yamada, H., Matsumoto, N., Kimura, M., 2004. Tonically active neurons in the primate caudate nucleus and putamen differentially encode instructed motivational outcomes of action. J. Neurosci. 24 (14), 3500–3510.
Yamada, H., Matsumoto, N., Kimura, M., 2007. History- and current instruction-based coding of forthcoming behavioral outcomes in the striatum. J. Neurophysiol. 98 (6), 3557–3567.
Yamada, H., Tymula, A., Louie, K., Glimcher, P.W., 2013b. Thirst-dependent risk preferences in monkeys identify a primitive form of wealth. Proc. Natl. Acad. Sci. U. S. A. 110 (39), 15788–15793.
Zald, D.H., Cowan, R.L., Riccardi, P., Baldwin, R.M., Ansari, M.S., Li, R., Shelby, E.S., Smith, C.E., McHugo, M., Kessler, R.M., 2008. Midbrain dopamine receptor availability is inversely associated with novelty-seeking traits in humans. J. Neurosci. 28 (53), 14372–14378.